Space-time species distribution modeling for opportunistic presence-only data: a case study of passerines in a protected area

Florian Lasgorceux, Julien Papaïx, Yoann Bunz, Damien Combrisson, Thomas Opitz

Space-time species distribution modeling for opportunistic presence-only data: a case study of passerines in a protected area

Florian Lasgorceux[1], Julien Papaïx[1], Yoann Bunz[2], Damien Combrisson[2], and Thomas Opitz[1]

https://doi.org/10.5802/fake.doi

Abstract

In recent decades, Europe has experienced a significant decline in common bird species, particularly farmland species, due to anthropic pressures like agricultural intensification. Protected areas, such as the Écrins National Park in France, play a crucial role in mitigating these impacts. In this study, we utilized an opportunistic presence-only dataset of passerine occurrences to evaluate the impact of protected areas on passerine trends. The data, gathered by skilled rangers from Écrins National Park, were used for spatio-temporal modeling to assess the target-group relative abundance of 76 passerine species across a regular grid, with aggregated occurrences per spatio-temporal cell serving as a proxy for sampling effort. The model demonstrated good calibration for most species, with AUC values from cross-validation scenarios exceeding 0.8 in most cases. The model also effectively distinguished habitat preferences and migratory status. Additionally, we compared trends in target-group relative abundance over 2001–2019 in the Écrins National Park with those across France using the French Breeding Bird Survey (STOC program) for 59 common species. Our analysis revealed that forest specialist species benefited the most from protected areas, farmland species decreased more slowly, and high-elevation specialist species generally decreased. Though, some results should be interpreted with care since our assumption of a homogeneous reporting rate across target-group species may be too strong for some very common species. Our findings illustrate that the extensive spatio-temporal resolution provided by opportunistic presence-only data offers valuable insights into biological phenomena and their trends, while reducing the need for other data sources to determine sampling effort proxies. Similar datasets from various protected areas could serve as powerful tools for assessing the effectiveness of conservation policies.

Keywords: Écrins National Park, INLA, habitat preference, migratory status, Poisson process, opportunistic presence-only data, relative abundance, sampling effort, spatio-temporal model, STOC program, target-group

[1]Biostatistics and Spatial Processes, INRAE, Avignon, France, [2]Parc national des Écrins, Domaine de Charance, Gap, France

Correspondence
florian.lasgorceux@proton.me

Introduction

In recent decades, Europe has seen a significant decline in the populations of common bird species (Inger et al., 2015), particularly those inhabiting agricultural landscapes (Donald et al., 2001). This sharp decline in farmland bird species has prompted extensive research, leading to numerous country-specific studies (Heldbjerg et al., 2018; Kamp et al., 2021; Newton, 2004; Reif et al., 2008b; Sanderson et al., 2013; Traba and Morales, 2019; Wretenberg et al., 2006). A large-scale study in Europe by Rigal et al., 2023 recently quantified the anthropic pressures impacting common bird abundance. They identified agricultural intensification, particularly the use of pesticides and fertilizers, as the primary factor contributing to the general decline, especially among invertebrate feeders. In contrast, responses to changes in forest cover, urbanization, and temperature showed greater variation among different species.

The conclusions regarding the health status of forest species in Europe are less consistent. Gregory et al., 2007 estimated that, on average, common forest birds declined by 13% and common forest specialists by 18% from 1980 to 2003. In contrast, by considering a different indicator over the period 1980-2015, Gregory et al., 2019 found a relative stability in common European forest bird populations. A possible explanation for these differences could be the migratory status of the species. Schulze et al., 2019 demonstrated that non-migratory forest bird species in Central Europe have shown significant positive population trends due to beneficial changes in forest management and environmental conditions. In contrast, birds migrating across continents have declined in recent decades, suggesting significant, contrasting changes in bird populations in Europe. Additionally, habitat preference plays a critical role. Reif et al., 2008a concluded that species closely associated with lowland broad-leaved forests have experienced more positive population trends, whereas those associated with montane and coniferous forests have shown more negative trends.

Finally, mountain bird species are particularly vulnerable, experiencing an average decline of 10% in Europe (Lehikoinen et al., 2019). This decline is driven by climate and land use changes, such as grazing pressure and afforestation, which have led to distribution shifts towards mountaintops. Studies by Flousek et al., 2015 and (Zamora and Barea-Azcón, 2015) support this, indicating that species breeding at higher altitudes are experiencing more negative population trends, with long-distance migrants being particularly affected.

Protected areas and conservation efforts play a crucial role in mitigating the decline of bird populations across Europe. According to the IPBES, 2019, conservation investments from 1996 to 2008 have resulted in an average reduction of 29% in the extinction risk for mammals and birds across 109 countries. Focusing on birds across Europe, the EU's Natura 2000 protected area network, while not preventing country-wide population declines in some threatened grassland bird species (Silva et al., 2018), has been effective for bird conservation, notably for threatened species (Duckworth and Altwegg, 2018). Studies by Barnes et al., 2023 also indicate positive associations between protected areas and bird abundance, particularly benefiting rare and declining species. Timmers et al., 2022 conducted a comprehensive meta-analysis and demonstrated a strong association between strict protection measures (International Union for Conservation of Nature [IUCN] categories I–IV) and higher bird occurrence in larger forest fragments.

In France, a National Park is formed of two zones with different regulatory statuses: the core (regulated area) - the national Park guarantees the protection of this area, as per its decrees, and manages any human activities carried out there, in line with its management objectives - and the

surrounding area (projects) - a space designed to achieve ecological consistency and solidarity with the National Park core. In this area, the National Park plays an advisory role and can act as a partner in projects to preserve and promote the natural, historic, cultural and landscape heritage -. The Écrins National Park is one of those protected areas. The park's geographic features include significant elevation changes, with several peaks over 4000 meters, extensive coniferous forests (especially larch), and numerous alpine pastures. The park is responsible for multiple biodiversity monitoring programs within its territory (Bunz, 2022), which have led to extensive synthesis and research works (Noël et al., 2023).

In addition to data from monitoring programs, the Écrins National Park possesses a large dataset of presence-only records collected opportunistically by rangers. The primary use of these data is to ensure ecological surveillance with broad spatio-temporal resolution and to serve as a basis for knowledge-sharing within the context of development projects. Using these data in statistical modeling presents a challenge due to sampling variability, which occurs in space and time, and between species and observers because of their opportunistic nature (Van Strien et al., 2013). This sampling variability translates into biases in species distribution models that do not account for it. In this study, we propose to harness this extensive dataset for modeling species habitat preferences, classifying species migratory status, and studying time variations in target-group relative abundance, meaning the relative abundance of a species against a pool of species constituting the so-called target-group of species.

Various estimation frameworks and algorithms exist for constructing species distribution models and calibrating their parameters from presence-only data. Widely used methods include Maxent, based on the maximum-entropy principle (Phillips et al., 2006), and various statistical regression modeling frameworks (Valavi et al., 2022). These methods are often based on point-process representations of data (Renner et al., 2015; Warton and Shepherd, 2010), where each observed occurrence of a species is viewed as a point in a cloud of points located in space and time. In this context, models such as Maxent and logistic regression are equivalent to a special case of the point-process setting (Fithian and Hastie, 2013; Renner and Warton, 2013). Due to the uncertainty in reported positions in the Écrins National Park dataset, we rather implement a degraded version of these point process models by aggregating occurrences into spatio-temporal cells, which leads to the use of a generalized additive regression model.

Random-effect modeling are often used to capture the complex spatio-temporal structures in data and ecological processes, accurately assessing various sources of uncertainty. This has led to the widespread adoption of Bayesian inference techniques such as Markov Chain Monte Carlo (MCMC, (Gilks et al., 1995; Link et al., 2002)) or Integrated Nested Laplace Approximations (INLA, Illian et al., 2013). We apply the INLA approach to perform complex Bayesian spatio-temporal inferences with relatively large datasets by combining generalized additive regression models with the Stochastic Partial Differential Equation (SPDE) approach, the latter used to represent spatial random effects (Lindgren et al., 2011). The construction and estimation of complex spatio-temporal ecological models are still recent developments (Belmont et al., 2024; Soriano-Redondo et al., 2019), and as far as we know, our study represents the first attempt to evaluate management policies of protected areas using solely opportunistic presence-only data for this type of model.

Material and methods

Data

Passerines presence-only data. The dataset of interest comprises 102,513 opportunistically reported events of passerine detections between 1994 and 2021, recorded by rangers of the Écrins National Park with professional skills in naturalistic expertise. We chose to focus our study on the *Passeriformes* because it is a taxon generally understood by all rangers, ensuring consistent reporting rates, unlike more specific taxa. Additionally, we have excluded three species – Common Raven (*Corvus corax*), Red-billed Chough (*Pyrrhocorax pyrrhocorax*), and Alpine Chough (*Pyrrhocorax graculus*) – due to the high uncertainty associated with their reported positions compared to the rest of the passerines. We narrowed the temporal window to the 1994–2021 period to ensure a minimum of 2000 reported events per year (see Appendix 1 for details).

The data were collected opportunistically, by sight and/or ear, without a predefined survey methodology, meaning that observation and reporting of observed individuals rely on the motivation of the rangers. Each row of the dataset contains a position, a date, the name of the reported species, the ID of the observer(s), and the number of individuals. However, we choose not to consider the number of individuals because it can vary greatly due to species behavior, particularly in gregarious species, and differences in observers' methods since some observers report species abundance, while others only note presence (see the eBird example in Horns et al., 2018). Thus, we consider one reported event as the presence of at least one reported individual, resulting in a total of 102,513 passerine occurrences.

Based on interviews with various rangers, we have gained insight that the reported position could be i) an approximation of the reported individual's position at detection time, ii) the observer's position at detection time, or iii) another, different position where the observer gathered several occurrences before adding them jointly to the data records. Though, when multiple occurrences are gathered at a station position, rangers ensure that the environment is consistent between the station position and the bird's individual position at detection time and that the distance between these two positions does not exceed 250m. This distance of 250m is obtained by considering at most 100m for the difference between the positions of the detected individual and the observer by sound recognition (Haupert et al., 2023), plus an additional 150m for the distance between the position at detection time and the station position. To account for this uncertainty surrounding the reported position, we aggregated the data by assigning each reported position to the center of a regular spatial grid with 500m resolution covering the Écrins National Park. We excluded boundary cells with an area smaller than 25m^2, which corresponds to the resolution of the environmental covariates we use for characterizing the spatial habitat preferences. This discretization results in dividing the Écrins National Park domain into 11,260 spatial cells.

Our objective is not only to infer species habitat preferences but also to analyze temporal trend variations in relative abundance. Therefore, we divided the 28 years of data into seven periods of 4 years each to capture long-term changes between such periods. Additionally, in order to take into account that some studied species are migratory, we further subdivided the data temporally by month to investigate intra-annual variations. This spatio-temporal discretization scheme results in a total of $7 \times 12 \times 11{,}260 = 945{,}840$ spatio-temporal cells.

Passerine population trends synthesis in France. To compare the local and national trends in relative abundance variations, we also utilized the French Breeding Bird Survey synthesis, known as the STOC program, for the period 2001–2019 (Fontaine et al., 2020; Jiguet et al., 2012). These data present the long-term abundance variation percentages of common birds in France during this period. Comparing trends from opportunistic data and STOC data serves three main purposes: (i) assessing the consistency of modeling assumptions, (ii) comparing local indicators within a protected area to global indicators across the territory of the entire country, and (iii) providing insights into space-time population trends for species specialized in mountainous habitats, for which surveys such as STOC are quite limited in terms of spatio-temporal coverage.

Environmental Data. The Écrins National Park is a high-mountain park where the terrain structure plays a predominant role in the ecosystems. We utilized the Digital Elevation Model data from RGE (IGN, 2018) to extract the elevation (McVicar and Körner, 2013) on a 5m regular grid. Subsequently, we calculated the slope at the same resolution using the 'terrain' function from the R package *terra* (Hijmans, 2024). Ultimately, we derived two spatial covariates: the mean elevation and the mean slope values per spatial cell at 500m resolution.

Regarding the land cover and land use data, we make use of the OSO dataset (Inglada et al., 2018). Originally at a resolution of 10/20m, we applied the nearest neighbor strategy to downscale the values to a 5m resolution, for alignment with the RGE data resolution. To avoid statistical issues due to uncommon land cover and land use types in the Écrins National Park, we aggregated data towards 10 representative categories: Urban, Crops, Meadows, Deciduous forest, Coniferous forest, Grasslands, Woody Heaths, Mineral Surfaces, Glaciers and snow, and Water (see Appendix 2 for further details). We then calculated the percentage of coverage of each category in each spatial cell at 500m resolution.

We also used the Historical Monthly Weather Data from WorldClim (CRU-TS 4.06 (Harris et al., 2020) downscaled with WorldClim 2.1 (Fick and Hijmans, 2017)) at 2.5 minutes spatial resolution (roughly 5km) between the years 1994 and 2021. The available variables were average minimum temperature (°C), average maximum temperature (°C), and total precipitation (mm). We extracted the corresponding values in each spatial cell, for each month, and each year. Since the inter-annual resolution of our spatio-temporal cells consists of periods of 4 years, we computed the mean of the extracted values of the 4 corresponding years for a given spatial cell and a given month. Finally, we removed the average minimum temperature covariate from our study due to its high correlation with the average maximum temperature (Pearson's $R > 0.99$).

Preprocessing of model covariates. Elevation shows strong variability in the Écrins National Park with certain climate and land cover configurations arising predominantly within specific elevation ranges. As a result, both land cover and climatic variables are correlated.

Hence, we began by decomposing the climatic variables into their spatial means and spatio-temporal anomalies with respect to their means. We then performed a Principal Component Analysis (PCA, Janžekovič and Novak, 2012) using the R package *ade4* (Dray and Dufour, 2007). The input variables were: the mean elevation, the mean slope, the percentages of coverage computed for each of the ten representative categories derived from the OSO classification, as well as the spatial means of average maximum temperature and total precipitation. The first 6 axes of the PCA, accounting for 75% of the information, allow for useful interpretation and have

therefore been incorporated into the species distribution models (Appendix 3). The first principal component axis explains a significant 31.1% of the variation in habitat types, primarily driven by high-elevation environments. , especially in steep areas. The third axis is influenced by grasslands, and the fourth axis is primarily driven by wetlands and glaciers. However, since we observe a significant predominance of bird occurrences in "Water" habitats within urbanized valleys (Figure 13 in Appendix 3) compared to "Glaciers and snow" habitats (751 occurrences versus 80), we interpret the fourth axis as 'urban wetlands". The interpretation of the fifth axis is also associated with high-altitude vegetation, as it is primarily driven by dense, low-growing shrubs and small trees; henceforth, we will refer to these environments as "woody heaths". The sixth axis is driven by low-elevation deciduous forests.

This results in the implementation of eight covariates in our statistical model: six spatial covariates from the PCA analysis replicated for each month and each period, and two spatio-temporal covariates defined as the anomalies of average maximum temperature and anomalies of total precipitation.

Statistical modeling

We applied the same Bayesian hierarchical model (Wikle, 2003) to each species with more than 100 occurrences over the period from 1994 to 2021, excluding *Bombycilla garrulus* where 90% of its 146 occurrences were reported in 2005, due to a brief invasion event of this species within the Écrins National Park that year. This resulted in a total of 76 species being analyzed.

Data model. We denote by s a spatial cell, by m a month, and by p a temporal period of 4 years, with (s, m, p) representing the corresponding space-time cell. The response variable, denoted as $Y_i(s, m, p)$, is the number of reported occurrences of species i from the opportunistic presence-only dataset. We model $Y_i(s, m, p)$ with a hierarchical generative additive mixed model (Knape, 2016; Pedersen et al., 2019) using a Poisson distribution:

$$Y_i(s, m, p) \mid \mu_i(s, m, p) \sim Poisson(\mu_i(s, m, p)), \tag{1}$$

where $\mu_i(s, m, p)$ is the average number of reported occurrences of species i in the cell (s, m, p).

We assume that $\mu_i(s, m, p)$ is obtained through the combination of two factors: (i) the abundance of species i in the cell (s, m, p), denoted by $\Lambda_i(s, m, p)$, and (ii) the sampling effort in cell (s, m, p) for species i, denoted by $E_i(s, m, p)$, which we assume to both act in a multiplicative way on $\mu_i(s, m, p)$ (Giraud et al., 2016). These relationships lead us to formulate the following equation:

$$\mu_i(s, m, p) = \Lambda_i(s, m, p) \times E_i(s, m, p) \tag{2}$$

Sampling effort. A major challenge is now to quantify or eliminate the term representing the sampling effort. When working with passerine bird survey data, parameters such as the number of listening points, the duration of time spent at each point, distances, study areas, *etc.*, are predefined and meticulously recorded. This ensures that data sampling remains consistent across different zones or years. With opportunistic data, this is not the case. Worse, sampling methods differ among observers, causing variations in the frequency of species reporting. This occurs because observers have the freedom to report sightings as they wish, resulting in significant differences in detection rates between observers and species. If not taken into account in the statistical modeling, this heterogeneous sampling will result in bias and wrong conclusions.

Within our spatio-temporal discretized framework, the first step is to obtain information about where and when no observations occurred. This helps distinguish between cells with zero occurrences due to the absence of observer presence and those with zero occurrences due to the absence of the species. The strategy involves utilizing the extensive opportunistic presence-only dataset, using reported occurrences of certain species as indicators of observer presence, as proposed by Botella et al., 2020. However, it is necessary to assume that these species are uniformly sampled by all the observers, corresponding to homogeneity in reporting rates across the species pool, as well as in the probability of detection. This explains one of our reasons to primarily restrict our study to passerines (see the Subsection *Passerines data*). Following existing literature, we refer to this set of chosen species with homogeneous sampling conditions as the target-group (TG) of species. Therefore, we denote the sampling effort term as E instead of E_i, and we write $\Lambda_{TG}(s, m, p)$ for the cumulative abundance of all species in the target-group in cell (s, m, p). We can then reformulate the average number of occurrences in terms of the abundance of species i compared to the cumulated abundance of the target-group, and the product of the sampling effort by the cumulated abundance of the target-group (Equation 4).

$$\mu_i(s, m, p) = \Lambda_i(s, m, p) \times E(s, m, p) \tag{3}$$

$$= \frac{\Lambda_i(s, m, p)}{\Lambda_{TG}(s, m, p)} \times \Lambda_{TG}(s, m, p) E(s, m, p). \tag{4}$$

To be able to statistically identify the first term that informs us about target-group relative abundance of species i, we now need a proxy of the second term $\Lambda_{TG}(s, m, p)E(s, m, p)$. The most natural approach is to use the number of reported occurrences of the target-group occurrences, denoted as $y_{TG}(s, m, p)$. We chose to use the combined occurrences of all passerine species, which was consistent with algorithms similar to that of Botella et al., 2020 since they were all selected except for 4 species observed only once [à modifier : (DOI, Data, scripts, code, supplementary materials).] We kept only the cells with at least one occurrence of the target group, reducing the number of studied cells to 32,486.

Target-group relative abundance. Employing a spatio-temporal distribution model enables the implementation of numerous spatio-temporally structured latent fixed or random effects within the linear structure that we will assume for the predictor $\log(\mu_i(s, m, p))$. We opted to use only one generic model for each of the 76 species to automate model fitting and facilitate inter-species comparisons. In Poisson models, it is common practice to distribute the Poisson intensity, denoted here as $\mu_i(s, m, p)$, using a log-link function to ensure that $\mu_i(s, m, p)$ remains positive. Focusing on the parameter of interest, the target-group relative abundance $\frac{\Lambda_i(s,m,p)}{\Lambda_{TG}(s,m,p)}$, we constructed our linear regressor by incorporating the proxy of the sampling effort, $y_{TG}(s, m, p)$, as an offset (Equation 5).

By studying the abundance of a passerine compared to all others, we compare species with different biological characteristics, such as habitats and migration status, which need to be taken into account in the linear regression. We denoted α_i as the intercept. We examined a linear effect of the spatial covariates $\mathbf{X}^{(PCA)}(s)$ (PCA components) and the spatio-temporal covariates $\mathbf{X}^{(anomalies)}(s, m, p)$ (anomalies of climatic covariates) to estimate habitat preferences of species i, relative to other passerines. The term $W_i^{(m)}(s)$, $m = 1, \dots, 12$, represents a monthly latent spatio-temporal Gaussian field. Concretely, this field aims to model intra-annual spatial variations not

captured by the covariates, typically variations in target-group relative abundance due to the migration of certain passerines within the territory of the Écrins National Park. Lastly, we denote by $f_i(p)$ a non-spatialized inter-annual effect, aiming to capture the variations in target-group relative abundance across each period p of 4 years.

$$\log(\mu_i(s,m,p)) = \log(y_{TG}(s,m,p)) + \log\left(\frac{\Lambda_i(s,m,p)}{\Lambda_{TG}(s,m,p)}\right) \quad (5)$$

$$= \log(y_{TG}(s,m,p)) + \alpha_i + \mathbf{X}^{(PCA)}(s)\beta_i + \mathbf{X}^{(anomalies)}(s,m,p)\gamma_i + W_i^{(m)}(s) + f_i(p). \quad (6)$$

Statistical inference. We employed the *INLA* package for the statistical inference of our models (Rue et al., 2009). INLA is a fast but accurate estimation method based on deterministic Laplace approximations –by contrast with approaches based on stochastic simulation, such as MCMC– and requires that the latent layer ($\log(\mu_i(s,m,p))$ in our model) follows a multivariate Gaussian distribution, possibly in very high dimension. In this setting, INLA enables the implementation of a wide range of Gaussian random effects, including spatial fields implemented through the SPDE approach, which provides a numerically convenient representation of the Matérn covariance function used routinely in spatial statistics (Lindgren et al., 2011), and of priors for hyperparameters such as variances or correlation ranges. In Appendix 4, we precisely describe the prior distributions of all parts of $\log(\mu_i(s,m,p))$, i.e., the structure of the model components before updating them with information from observation data to obtain their posterior distributions.

Validation and post-processing

The model presented previously is quite comprehensive, allowing for a thorough examination of information on a species-by-species basis. In the following sections, we delineate the post-processing phase undertaken to synthesize this information. We address questions pertaining to the model's validation and also delve into the three components of the linear predictor (Equation 6): those concerning the fixed effects – specifically, habitat preferences compared to the target-group denoted by β_i and γ_i; the spatial intra-annual component, characterized by the month-dependent Gaussian field W_i^m, which is associated with migratory status; and the inter-annual component, represented by the random i.i.d. Gaussian effect $f_i(p)$, which captures long-term trends in target-group relative abundance.

Computational cost. For each species, the model comprises 32,486 space-time cells with observations, and a total of 7,676 latent variables to estimate across the prediction cells. We conducted analyses using the R programming language (R Core Team, 2024) and utilized version 24.02.09 of INLA (Rue et al., 2009), leveraging the PARDISO 8.2 library to accelerate computations (Eftekhari et al., 2021; Gaedke-Merzhäuser et al., 2023; Pasadakis et al., 2023). This configuration typically yields computation times averaging around one minute for each model fit on an 11th Gen Intel(R) Core(TM) i7-1165G7 @ 2.80GHz processor.

Validation. We evaluated whether our model effectively extracted meaningful insights from the opportunistic data by comparing its predictive performance against a baseline that considered only sampling effort. We focus on the prediction of the binary event of presence or absence of a species in a given cell and month and compute the Area-Under-the-Curve (AUC,Fawcett, 2006; Jin Huang and Ling, 2005) (where the curve is the so-called Receiver Operating Characteristic curve) as a simple scalar prediction score for each species using two predictors: (i) the sampling effort proxy offset and (ii) the full linear predictor (Equation 6). Next, we assessed the model's

generalization ability for predicting new data using k-fold, spatial, and temporal cross-validation scenarios. In k-fold cross-validation, the dataset is divided into k equal parts, with one part used for validation while the rest is used for training (Jung, 2018). This approach yields $k + 1$ AUC scores per species: k scores from predicting each part separately, and one from predicting the entire dataset. We selected $k = 10$ to ensure comparability with temporal and spatial scenarios, where the training data represented between 3.9% and 13.7% of the total volume. This choice aimed to maintain consistency in the quantity of test data across scenarios, ensuring equitable evaluation conditions. In the spatial scenario, we assessed model robustness by alternately removing all spatio-temporal cells within a given municipality of the Écrins National Park. Seven municipalities were selected based on geographic zones and data availability, resulting in seven AUC scores per species. For the temporal scenario, we alternately randomly removed half of the data for a given period, resulting in seven AUC scores per species. Further details on the size of the training datasets are given in Appendix 5.

Fixed effects. We estimated the *a posteriori* distribution of coefficients β_i and γ_i separately for each species i (Equation 6). The posterior mean of each parameter and its sign quantify the importance of the covariates in explaining occurrences of species i relative to the occurrences of all the passerines taken together. The credibility interval of each parameter helps determine how strongly the corresponding covariate influences the species; if the interval does not contain zero, we can consider the covariate as being "significant" (by analogy with the frequentist notion of significance). To synthesize the estimated mean coefficients and assess parameter similarities across species occupying comparable ecological habitats, we conducted Principal Component Analysis (PCA) on estimated parameters followed by species clustering based on the estimated mean effects. This clustering was performed using a hierarchical agglomerative clustering (HAC) algorithm implemented through the *hclust* function, employing the *ward.D2* method (Murtagh and Legendre, 2014).

Month-based spatio-temporal Gaussian field. The month-based spatio-temporal Gaussian field $W_i^{(m)}$ adds flexibility to the model but is challenging to summarize graphically since we have 12 maps per species. Therefore, we opted to reduce dimensionality by spatially averaging each field. For each species, this yields a curve of 12 points depicting the intra-annual variations in occurrences relative to the target-group. Instead of plotting all 76 curves on a single graph, we conducted a Functional Principal Component Analysis (FPCA, Ramsay and Silverman, 2005). The mechanism of the approach is analogous to PCA but adapted to functions instead of vectors. In our case, FPCA decomposes the intra-annual mean effect of a given species into (i) the mean intra-annual effect across all species plus (ii) the remaining signal represented by scores associated with empirically identified harmonics. In a functional principal component analysis (FPCA), harmonics represent the most significant modes of variation in the observed functions. These harmonics are akin to principal components in traditional PCA but are applied to functions rather than conventional variables, where the difference is that functions are represented as vectors with a very large number of components (larger than the sample size of functions), and typically show correlation for components at near positions within the vector. We utilized the *fda* package to conduct these analyses (Ramsay et al., 2009).

Inter-annual effects. Our motivation for introducing the inter-annual effect in the linear predictor (Equation 6) lies in comparing the target-group relative abundance trends of passerines in the

Écrins National Park with the relative abundance trends of common birds in the STOC. If we denote $\lambda_i^{(STOC)}(y)$ as the estimated abundance of species i in year y by the STOC, then the percentage variation in abundance computed by the STOC (Fontaine et al., 2020) can be expressed as:

$$\left(\hat{\lambda}_i^{(STOC)}(2019) - \hat{\lambda}_i^{(STOC)}(2001)\right) \times \frac{100}{\hat{\lambda}_i^{(STOC)}(2001)}.$$

In the model presented in Equation 6, the term capturing the effect of the period p on the target-group relative abundance of species i is $\exp(f_i(p))$. The INLA method allows us to estimate a posterior distribution of each $\exp(f_i(p))$. To mimic the STOC period of study, we assume the target-group relative abundance to be constant in each period p. This allows us to attribute an estimated relative effect $f_i(y)$ to each year y between 2001 and 2019. We then calculated a regression line using a linear model with the $f_i(y)$ as the response variable and y the explanatory variable. If we denote $\hat{f}_i^{(ENP)}(y)$ the fitted value of this linear regression, we could calculate the percentage variations in target-group relative abundance of species i as

$$\left(\hat{f}_i^{(ENP)}(2019) - \hat{f}_i^{(ENP)}(2001)\right) \times \frac{100}{\hat{f}_i^{(ENP)}(2001)}.$$

To enhance robustness and take into account statistical uncertainty, we generated 1000 posterior distributions for each target-group relative abundance trend parameter and repeated this procedure. Then, we used the median percentage variation in target-group relative abundance as a reference for each species and compared it to the STOC.

Results

Validation

Figure 1 displays the boxplots of AUC values computed species by species as described in section *Validation and post-processing*. We notice a clear improvement in AUC when using the full linear predictor compared to using only the sampling-effort proxy as offset. This confirms that opportunistic data are not solely constrained by sampling methods and that valuable information can be extracted from them.

Regarding the boxplots of AUC values obtained using cross-validation (with one value for each hold-out dataset), we observe a few outliers among the species, some of which occur in all scenarios, as it is the case for *Cinclus cinclus* and *Motacilla cinerea*. These two species with poor AUC values relative to others are stream specialist species, for which covariates do not capture the habitat well. It is worth noting that a species appearing multiple times as an outlier within the same scenario is listed only once for readability.

The AUC values of models with cross-validation are typically slightly lower than those without cross-validation, as expected due to the reduction in the amount of training data and the more challenging prediction setting with new data not used during training. However, they remain generally stable, suggesting that the model does not overfit. Furthermore, despite this relative decrease, the AUC values generally remain high, with approximately 75% of AUC values above 0.8 across all scenarios. Consequently, we conclude that the model demonstrates a very good fit to the data, except for two species: *Cinclus cinclus* and *Motacilla cinerea*, which we have excluded from further analysis.

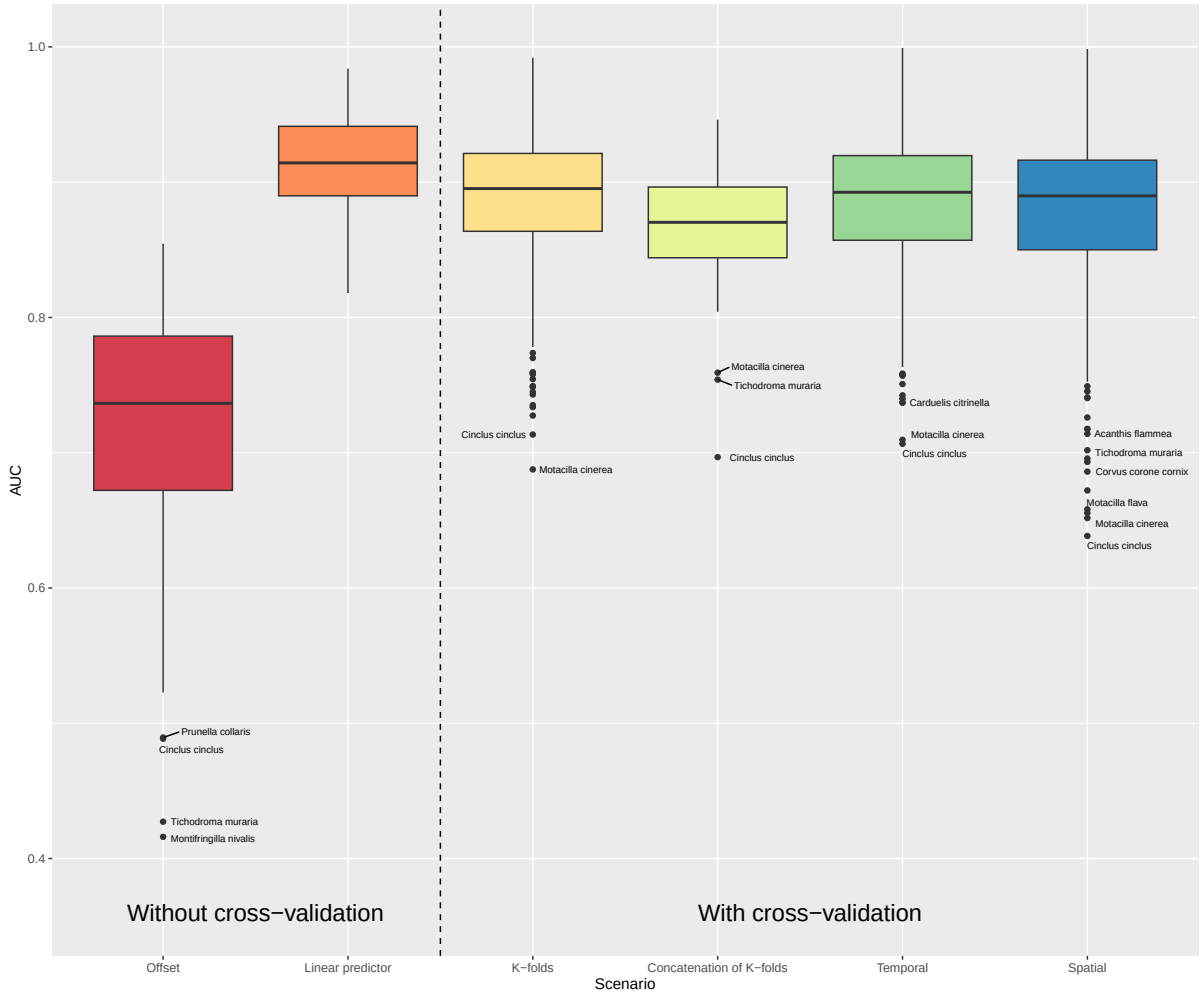

Figure 1 – AUC values calculated based on various linear-predictor and cross-validation scenarios. Boxplots summarize the set of AUC values for all species, and in the case of cross-validation for each combination of species and hold-out dataset. Notations are as follows: "Offset" – model where linear predictor contains only the offset; "Linearpredictor" – model with full linear predictor; "K-folds" – model fitted by randomly removing 10% of the cells, ten times; "Concatenation of K-folds" – AUC values computed by concatenating the predictions of the K-folds scenarios; "Temporal" – model fitted by randomly removing half of the data in a given time period, for each time period; "Spatial" – model fitted by removing all the data which occurred in a given city, for seven cities. The species with multiple outlier AUC values in "K-folds", "Temporal" and "Spatial" scenarios are only noted once. Details on the four cross-validation scenarios (where models always have the full linear predictor) can be found in the "Post-processing and Validation - Validation" section.

Fixed Effects

The mean estimated effects of each covariate and their significance are detailed in Tables 5-7 in Appendix 6. To summarize the information on habitat spatial covariates, we provide a classification into three clusters based on Principal Component Analysis conducted on the estimated mean coefficients for each habitat spatial covariate (see subsections "Data - Covariates" and "Validation and Post-processing - Fixed Effects"). We did not include any species with less than two significant covariates since we consider that the model does not provide enough information on them. These species are generally those with very few occurrences, as 10 out of these

11 species have fewer than 551 occurrences over the 28 years of data, where the value 551 is below the 25th-percentile of species occurrences. The list of removed species is given in Table 8 in Appendix 6. The PCA reveals two principal axes explaining 62.2% of the classification: the first axis distinguishes vegetated habitat (coniferous and deciduous forests VS urban wetlands), while the second axis highlights an altitudinal gradient.

The three clusters are presented in Figure 2. We interpret them as follows. Cluster 1: Species mostly found in closed habitats such as coniferous and deciduous forests (green); Cluster 2: Species mostly found in high-elevation environments (orange); Cluster 3: Species mostly found in open habitats and valleys (violet). These results are coherent when comparing a map of elevation with a map of clusters with the highest occurrences on a 500m$\times$500m regular grid in the Écrins National Park (see Figure 14 in Appendix 6).

The ellipse associated with forest species represents an altitudinal gradient, with species found in low-elevation forests (*Pyrrhula pyrrhula*), to medium (*Anthus trivialis*) and high-elevation forests (*Turdus torquatus)*. We also observe this altitudinal gradient in the cluster associated with species from open habitats and valleys, with rocky habitat species such as *Tichodroma muraria* and *Phoenicurus ochruros*, at the boundary of the high-altitude species cluster. The cluster associated with species specialized to high-elevation habitats is smaller but well-defined, with typical species such as *Prunella collaris* and *Montifringilla nivalis*.

To address the spatio-temporal covariates, we began by examining their impact on the linear predictor across all species. We computed the standard deviation of each covariate $X_j \in \mathbf{X}^{(PCA)}$ (and $\mathbf{X}^{(anomalies)}$), multiplied by the mean estimated associated parameter $\beta_{i,j}$ (or $\gamma_{i,j}$) for each species, and then averaged these values. Our analysis revealed that the precipitation anomalies covariate had the smallest impact on the linear predictor, with a Mean(SD) of 0.09. This finding was further supported by only 12 species exhibiting a significant parameter associated with precipitation anomalies. In contrast, the temperature anomalies covariate had a substantial effect on the linear predictor, with a Mean(SD) of 0.52, which is significant when compared to the elevation PCA axis (Mean(SD) = 0.79). Notably, 45 species demonstrated a significant parameter associated with maximum temperature anomalies. Among these, we identified species with positive parameters—indicating they tend to be more prevalent when deviations in maximum temperatures from the mean are positive—such as *Emberiza hortulana* and *Lanius collurio*. Conversely, we also identified species with negative parameters—indicating they are more frequently observed when deviations in maximum temperatures from the mean are negative—such as *Coccothraustes coccothraustes* and *Fringilla montifringilla*. These results align with the ecological characteristics of these species, confirming that thermophilic species thrive in warmer conditions, while cold-resistant species are more abundant in cooler conditions.

Intra-annual effect

The first two extracted harmonics encompass a significant portion of the intra-annual variability, explaining 83% of the variance. While the primary harmonic exhibits a greater positive effect during winter months compared to summer months, the second harmonic shows a positive effect in summer months and a negative effect in winter months (see Figure 15 in Appendix 7). Consequently, species with positive scores on the first harmonic tend to be overrepresented in winter, whereas species with positive scores on the second harmonic are more likely to be overrepresented in spring and summer, which hints at a potential link with the migratory status of species.

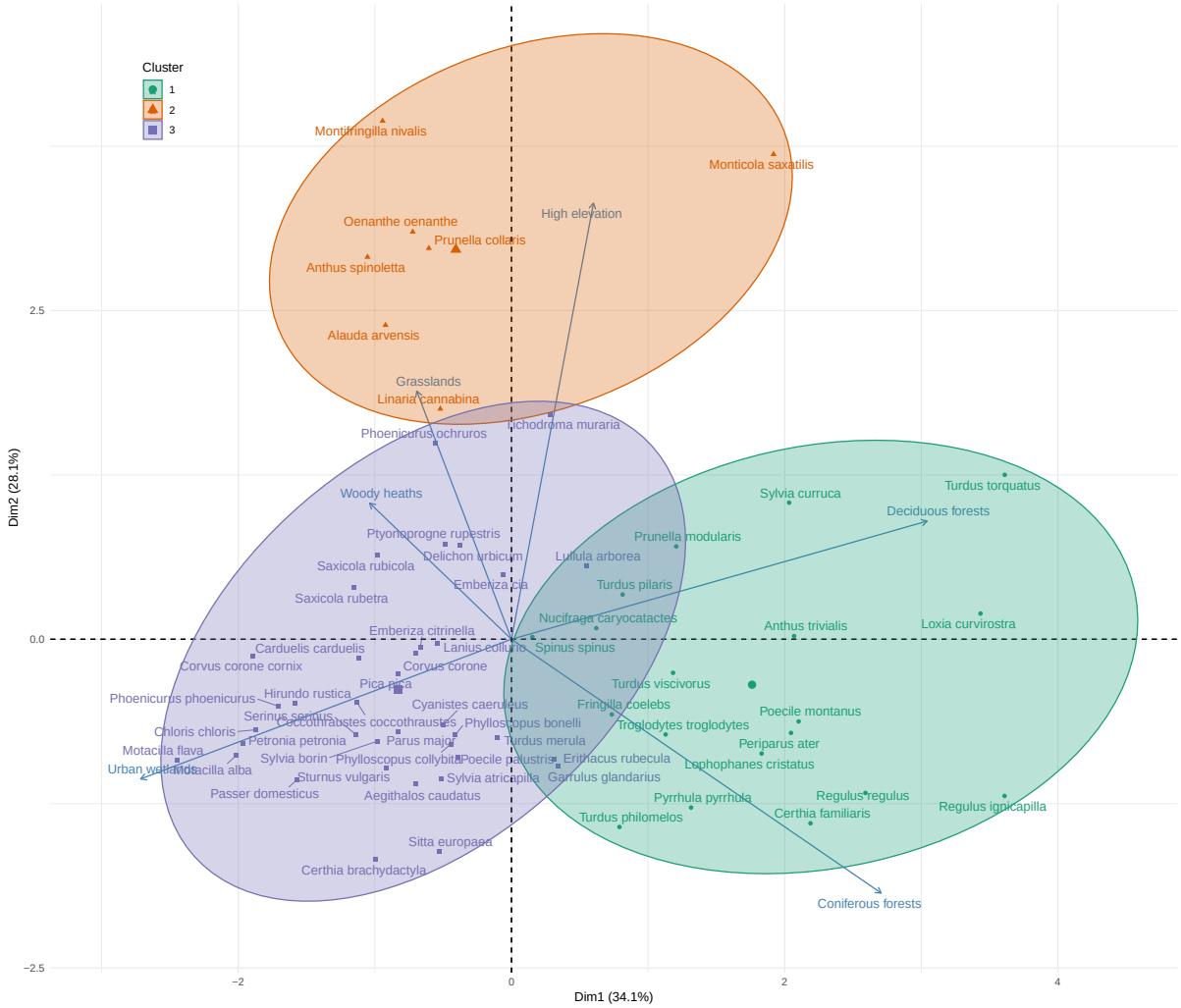

Figure 2 – Classification of 63 species in three clusters based on the estimated mean effects of spatial covariates. A Principal Component Analysis was conducted on the species with at least two credibility intervals that do not include 0. The two main axes explain 62.2% of the variance. Cluster 1: Species mostly found in closed habitats such as coniferous and deciduous forests (green); Cluster 2: Species mostly found in high-elevation environments (orange); Cluster 3: Species mostly found in open habitats and valleys (violet).

Figure 3 illustrates the scores associated with the two first harmonic for each species, categorized by migratory status within the territory of the Écrins National Park, as provided by experts from the park. Colored ellipses are provided for readability. This analysis confirms that species overrepresented in winter and underrepresented in spring and summer primarily consist of sedentary species, while those underrepresented in winter and overrepresented in spring and summer correspond to migratory species. The details of the scores for each species are given in Table 9 in Appendix 7. These harmonics effectively distinguish between sedentary and migratory species within the Écrins National Park, affirming that the month-based spatio-temporal Gaussian field $W_i^{(m)}$ adequately accounts for spatial and intra-annual species variations not explained by the physical covariates across the territory.

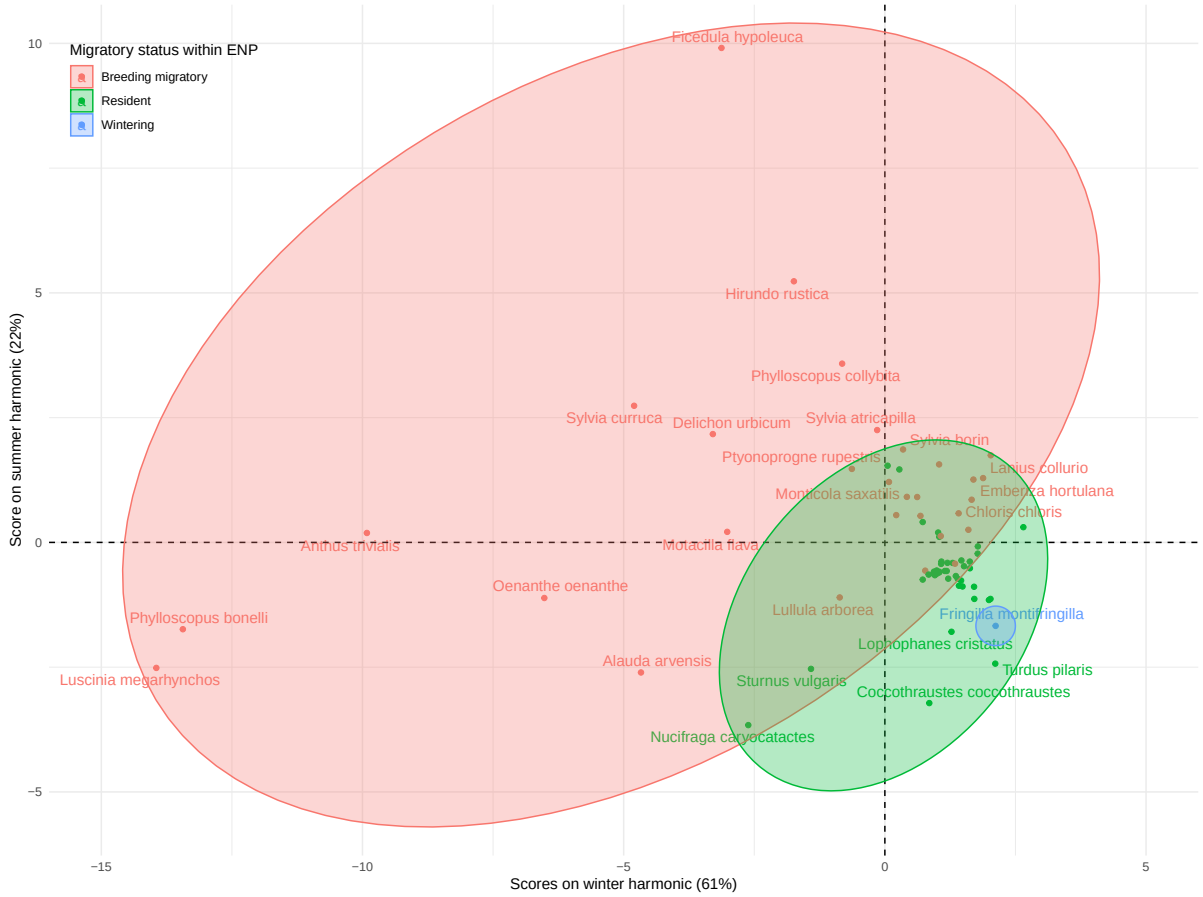

Figure 3 – Point plot of scores associated with the first two harmonics of the FPCA computed on the month-based spatio-temporal Gaussian field $W_i^{(m)}$ estimated for each species. The two first harmonics explain 83% of the variance. The species are categorized by their main migratory status within the territory of the Écrins National Park (ENP), as provided by experts from the park: breeding migratory (red); resident (green); wintering (blue).

Inter-annual variability and STOC comparison

The estimated percentage variations in target-group relative abundance in the Écrins National Park between 2001 and 2019, based on 1000 *a posteriori* samples, are illustrated in Figure 4. Species associated with high-elevation habitats exhibit a mean decline of -16.5% in target-group relative abundance during 2001–2019. This is mainly due to the strong decrease of three species: *Monticola saxatilis* (-53.5%), *Prunella collaris* (-26.4%) and *Montifringilla nivalis* (-23.4%). Conversely, species affiliated with the forest cluster experienced a growth of 12.4% over the same period.

Figure 4 shows that, out of the 19 forest species, 6 exhibited a positive trend while only 2 showed a negative trend based on the 95% credibility interval. For comparison, it is noteworthy that the STOC reported a decrease of 9.7% in abundance for specialist forest species in France. When focusing specifically on passerines considered forest specialists by the STOC, the difference becomes even more pronounced, with a growth of 23.2% in the Écrins National Park, while the STOC observed a growth of 2% for these species during the same period in France. It is important to note that this percentage is nevertheless skewed by *Regulus ignicapilla*, which shows a growth of 168% in relative abundance over the period.

Species linked to the valleys cluster experienced a mean decrease of -3.2% in target-group relative abundance. However, comparing this figure with STOC trends is challenging due to the mix of generalist species with specialists of built and agricultural environments within this cluster. To address this, we compare below the trends of passerines in the Écrins National Park, classified by the STOC as generalist species or species specialized in built and agricultural environments, with our estimated trends in target-group relative abundance. Built-environment passerines demonstrate stability in the Écrins National Park (0.26%) compared to a slight decrease in France (-5.68%). Generalist passerines show an increase of 7.4% in target-group relative abundance in the park, aligning with the 7% growth reported by the STOC for these species (and 19.4% for generalist common birds, not only passerines). For farmland species, both show a decrease, but at a slower rate of -16.5% compared to -22.6% (and 29.5% for farmland common birds, not only passerines).

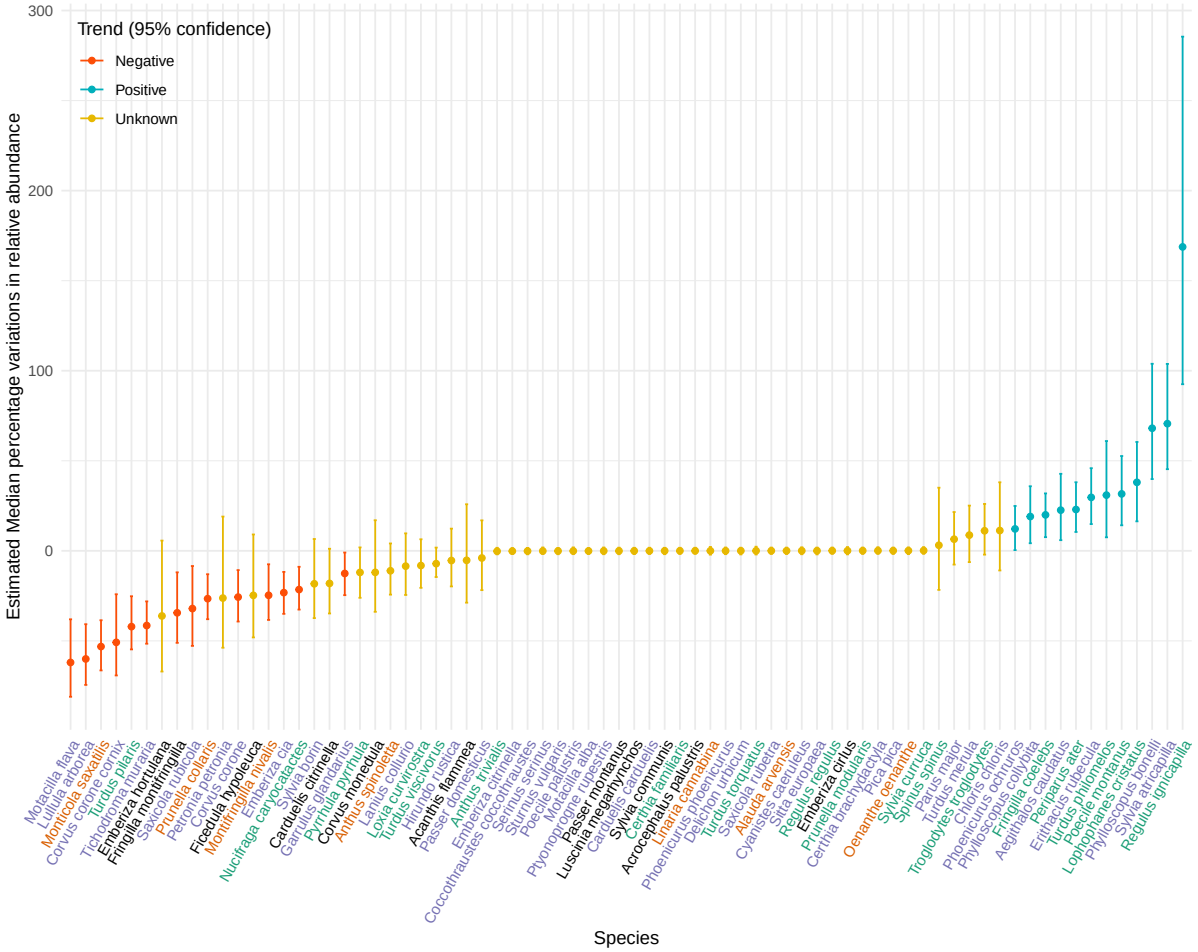

Figure 4 – Illustration of the estimated median percentage variations in target-group relative abundance and credibility intervals for 74 retained species in the Écrins National Park spanning the period 2001–2019. These trends are derived from 1000 samples of the *a posteriori* distribution of the inter-annual effect $exp(f_i(p))$. Details can be found in the "Post-processing and Validation - Inter-annual effects" section. Credibility intervals shown in red (respectively blue) correspond to intervals below (respectively above) zero, while yellow intervals include zero. Species names are color-coded according to their cluster affiliation in Figure 2. Species with fewer than two significant covariates were not classified and are shown in black.

Figure 5 displays more precisely the percentage variations of target-group relative abundance in the Écrins National Park against the percentage variations of abundance in France computed by the STOC, between 2001 and 2019. More details on the trends are given in Table 10, Appendix 8. Each species lies in one of the four quadrants. Quadrants (ii) and (iii) correspond to species whose trends locally within the Écrins National Park align with those in France: increasing for quadrant (ii) and decreasing for quadrant (iii). Quadrant (i) corresponds to species trending upward nationally but downward in the Écrins, whereas quadrant (iv) represents species increasing in the Écrins but decreasing nationally. The number of species in each quadrant is as follows: 8 for (i), 14 for (ii), 24 for (iii) and 14 for (iv). Quadrant (iv) is primarily composed of forest species, while quadrant (i) consists mainly of generalist species, particularly common ones.

Furthermore, while the national park status does not prevent the decline of certain species, it is noteworthy that for 38 species out of 60, trends are more favorable within the national park compared to national trends for all of France as represent by the $y = x$ slope in Figure 5. However, some species for which this is not the case are very common (quadrant (i)) and may be subject to reporting bias (see Discussion).

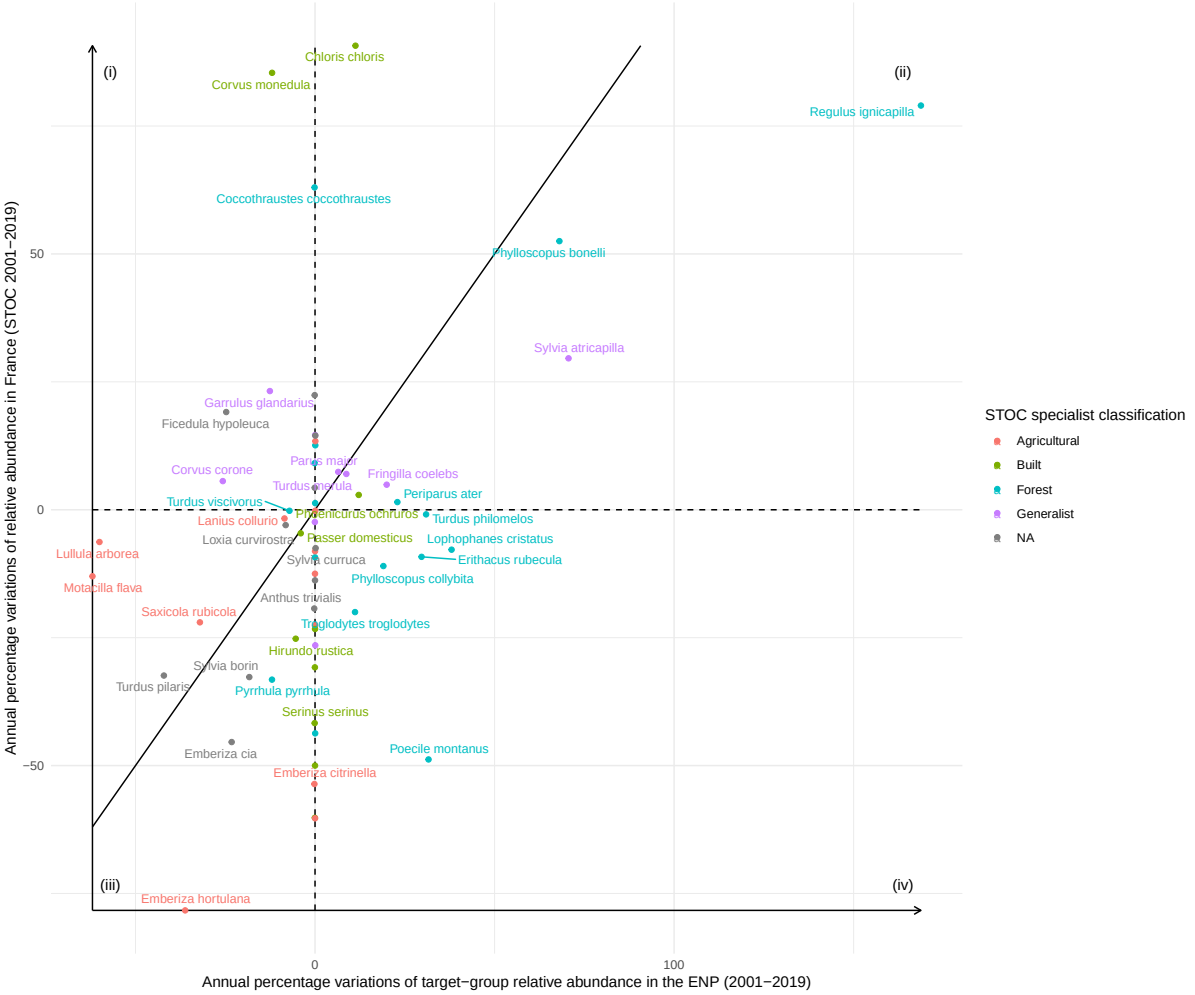

Figure 5 – Point plot of the estimated median percentage variations of target-group relative abundance in the Écrins National Park between 2001 and 2019, against the percentage variations of relative abundance in France between 2001 and 2019 computed by the STOC for 60 species. The names of species with less than 0.1% variation in target-group relative abundance are not plotted for readability.

Discussion

In our study, we demonstrated that under the assumption of sampling homogeneity across species (but where sampling effort is still allowed to vary in space and time), opportunistic presence-only data could be leveraged to estimate habitat preferences, migratory status, and target-group relative abundance trends of passerine species. This finding is not novel *per se*, as numerous studies have utilized such data to model species distributions or abundance trends (Botella et al., 2020; Bradter et al., 2018; Kéry et al., 2010; Phillips et al., 2009; Valavi et al., 2022; Van Strien et al., 2013). However, it is one of only a few approaches achieving this within a unique spatio-temporal model. To our knowledge, the most similar work has been done by Giraud et al., 2016 and Coron et al., 2018 modeling spatial relative abundance (abundance divided by the abundance of an arbitrarily chosen cell) of passerines using a Poisson distribution. Their work provides theoretical results regarding parameter identifiability, as well as scenarios for data simulation and parameter estimation. However, the use of their models requires access to appropriate survey data based on a standardized sampling protocol, whereas our study relied solely on a single set of opportunistic data. We also found the inclusion of the month-based spatio-temporal latent Gaussian field $W_i^{(m)}$ and the use of Functional Principal Component Analysis to be pertinent for assessing phenological effects when modeling target-group relative abundances of species with different migratory statuses. Another potential application of such Gaussian fields and FPCA could involve implementing a nonlinear additive predictor component for altitude to study species' phenological changes as responses to climate: altitude ascents, migrations, *etc.*

The STOC has demonstrated the effectiveness of public policies on protected areas. Outside of reserves, the average decline of 56 species between 2004 and 2018 was -6.6%, whereas within reserves, an increase of 12.5% was observed (Fontaine et al., 2020). Additionally, our study offers new insights into the role of protected areas in mitigating the decline of passerine populations, though our trends should be interpreted with caution. Indeed, several very common species show a negative estimated target-group relative abundance in the park, while the STOC indicates positive trends for these same species. Thus, we believe that our assumption of homogeneous reporting is overly optimistic and partially inaccurate. Despite this issue affecting 7 out of 60 species, we can still draw meaningful conclusions.

Notably, we demonstrate that forest passerines benefit the most in the Écrins National Park. While not reversing the trend, the decline of farmland passerines in the park is slower than in the rest of France, consistent with findings from previous studies (Palacín and Alonso, 2018; Silva et al., 2018). Furthermore, our study provides novel insights into high mountain species not previously investigated by the STOC. Our indicator, the target-group relative abundance, shows a global decline for species specialist to high-elevation environments. This trend aligns with the global decrease of mountain specialist species in Europe (-10% during 2002–2014) as reported by Lehikoinen et al., 2019. These findings will be valuable for comparison with upcoming analyses of the STOM, a survey analogous to the STOC for mountain species, which has only been operational since 2012, with its first results yet to be analyzed.

We identify three areas for future improvements in our modeling approach using solely opportunistic data:

(i) The assumption of uniform sampling, which could be questionable due to differences in detectability, species commonness/rarity (Snäll et al., 2011), or agent identification skills and reporting prevalence (Bradter et al., 2018), albeit reasonable in practice and lacking better options.

Heterogeneous detectability remains an issue without data based on standardized sampling protocols and seems difficult to correct except for trying to include prior expert knowledge into models. Different reporting behavior due to species commonness/rarity can introduce bias in estimated intercept terms, such as α_i in Equation 6, but would not have any impact on the other terms varying in space and/or time, as long as this bias in reporting behavior is homogeneous across space, time and physical predictors. Effects related to agent identification skills and reporting prevalence could potentially be identified by including random effects for the rangers in the model. As a general recommendation to reduce biases and improve the exploitability of opportunistic presence-only data, we suggest that when observers report a species, all species of the same taxon should also be reported for better use of opportunistic presence-only data in species distribution modeling.

(ii) The acquired information is relative to a target-group of species since we used the target-group occurrences as a proxy for the sampling effort (Equation 4). This implies that the potential for interpretations of results in terms of absolute abundance and its variation across covariates, space, and time remains relatively limited.

(iii) There are multiple ways to define this target-group, which impacts the interpretation of abundances relative to it. The composition of this target-group primarily relies on available data sources, ranging from studies covering a single species (Farr et al., 2021) to those encompassing thousands (Botella et al., 2021). Some studies focus exclusively on species within the same taxonomic group (Van Strien et al., 2013), while others consider species across different taxa (Escamilla Molgora et al., 2022). Botella et al., 2020 recommends choosing a set of species that are consistently abundant across a broad range of environmental sub-regions, that we did in this study.

We have recognized a pressing need for more comprehensive descriptions of what we refer to as "sampling effort" when dealing with opportunistic presence-only data, and for methodologies to effectively incorporate it into modeling endeavors. Various strategies have been proposed to address sampling efforts depending on the studied taxa, the available datasets and the type of model. These include the utilization of random or target-group pseudo-absences with Maxent (Phillips et al., 2006, 2009), target-group background occurrences (Botella et al., 2020), integration of information from detection/nondetection data (Dorazio, 2014; Fithian et al., 2015; Giraud et al., 2016), or questionnaires (Bradter et al., 2018). Additionally, consideration of proxy variables such as road density or population density (Kervellec et al., 2023), and covariates representing the accessibility of a site, such as distance to roads, cities, coastlines, and protected areas (El-Gabbas and Dormann, 2018; Henckel et al., 2020; Moreira et al., 2024; Warton et al., 2013) or refinements between these methods and the target-group approach (Chauvier et al., 2021). Another commonly used proxy, especially in studies focusing on cetaceans and fish, is the logbooks of vessels (Alglave et al., 2022; Ver Hoef et al., 2021).

Our findings suggest that, despite the statistical challenges arising from taking sampling biases into account, opportunistic presence-only data provide unparalleled spatio-temporal coverage, allowing for the depiction of consistent biological indicators that would be challenging to obtain using traditional methods. This includes monitoring trends in target-group relative abundance over extended periods and developing species distribution models across vast geographical areas. Such information can serve as valuable quantitative indicators for assessing the effectiveness of conservation policies in protected areas.

In our case study, very large occurrence numbers were available for the target-group, such that uncertainties about the target-group abundance can be expected to be relatively small. For modeling more precisely the target-group abundance, for example in cases with smaller occurrence numbers or when large areas of the study domain are only very weakly sampled, we could develop an alternative approach wherein $Y_{TG}(s, m, p)$ could be initially modeled with a Poisson distribution using a mean parameter $\mu_{TG}(s, m, p)$, fitted to the data to estimate $\mu_{TG}(s, m, p)$. Subsequently, we would use the estimated Poisson mean as a proxy for $\Lambda_{TG}(s, m, p)E(s, m, p)$, rather than the raw count. This modification could potentially enhance robustness and improve the assessment of uncertainties inherent to our modeling approach.

Acknowledgements

The authors would like to thank all the staff of the Écrins National Park and its scientific team for contributing to the dataset. They also appreciate advice of Denis Allard on using factorial principal component analysis, and Loïc Houde for technical support with the high-performance computing cluster used to implement the models of this case study.

Fundings

The authors declare that they have received no specific funding for this study.

Conflict of interest disclosure

The authors declare that they comply with the PCI rule of having no financial conflicts of interest in relation to the content of the article.

Data, script, code, and supplementary information availability

Data are available online (https://doi.org/10.24072/fake1[Replace by the DOI of the webpage hosting the data]; cite[Replace by the citation of the data])
Script and codes are available online (https://doi.org/10.24072/fake2[Replace by the DOI of the webpage hosting the script and code]; cite[Replace by the citation of the script and code])
Supplementary information is available online (https://doi.org/10.24072/fake3[Replace by the DOI of the webpage hosting the Supplementary information]; cite[Replace by the citation of the Supplementary information])
The DOI hyperlinks should be active. They should also be present in the reference list and cited in the text. For the reference section below, do not forget to add a doi for each reference (if available). Do not forget to add the reference of the recommendation, the reference of the data, scripts, code and supplementary material to your bib file, if appropriate.

References

Alglave B, Rivot E, Etienne MP, Woillez M, Thorson JT, Vermard Y (2022). *Combining scientific survey and commercial catch data to map fish distribution*. *ICES Journal of Marine Science* **79**, 1133–1149. https://doi.org/10.1093/icesjms/fsac032.

Barnes AE, Davies JG, Martay B, Boersch-Supan PH, Harris SJ, Noble DG, Pearce-Higgins JW, Robinson RA (2023). *Rare and declining bird species benefit most from designating protected areas for conservation in the UK*. *Nature Ecology & Evolution* **7**, 92–101. https://doi.org/10.1038/s41559-022-01927-4.

Belmont J, Martino S, Illian J, Rue H (2024). *Spatio-temporal Occupancy Models with INLA*. https://doi.org/10.48550/arXiv.2403.10680.

Botella C, Joly A, Bonnet P, Munoz F, Monestiez P (2021). *Jointly estimating spatial sampling effort and habitat suitability for multiple species from opportunistic presence-only data*. *Methods in Ecology and Evolution* **12**, 933–945. https://doi.org/10.1111/2041-210X.13565.

Botella C, Joly A, Monestiez P, Bonnet P, Munoz F (2020). *Bias in presence-only niche models related to sampling effort and species niches: Lessons for background point selection*. *PLOS ONE* **15(5)**, e0232078. https://doi.org/10.1371/journal.pone.0232078.

Bradter U, Mair L, Jönsson M, Knape J, Singer A, Snäll T (2018). *Can opportunistically collected Citizen Science data fill a data gap for habitat suitability models of less common species? Methods in Ecology and Evolution* **9**, 1667–1678. https://doi.org/10.1111/2041-210X.13012.

Bunz Y (2022). *Les programmes scientifiques de la faune vertébrée*. Parc national des Écrins, Domaine de Charance, Gap, France, p. 423. URL: https://www.documentation.eauetbiodiversite.fr/notice/les-programmes-scientifiques-de-la-faune-vertebree-edition-20220.

Chauvier Y, Zimmermann NE, Poggiato G, Bystrova D, Brun P, Thuiller W (2021). *Novel methods to correct for observer and sampling bias in presence-only species distribution models*. *Global Ecology and Biogeography* **30**, 2312–2325. https://doi.org/10.1111/geb.13383.

Coron C, Calenge C, Giraud C, Julliard R (2018). *Bayesian estimation of species relative abundances and habitat preferences using opportunistic data*. *Environmental and Ecological Statistics* **25**, 71–93. https://doi.org/10.1007/s10651-018-0398-2.

Donald PF, Green RE, Heath MF (2001). *Agricultural intensification and the collapse of Europe's farmland bird populations*. *Proceedings of the Royal Society of London. Series B: Biological Sciences* **268**, 25–29. https://doi.org/10.1098/rspb.2000.1325.

Dorazio RM (2014). *Accounting for imperfect detection and survey bias in statistical analysis of presence-only data*. *Global Ecology and Biogeography* **23**, 1472–1484. https://doi.org/10.1111/geb.12216.

Dray S, Dufour AB (2007). *The ade4 Package: Implementing the Duality Diagram for Ecologists*. *Journal of Statistical Software* **22**, 1–20. https://doi.org/10.18637/jss.v022.i04.

Duckworth GD, Altwegg R (2018). *Effectiveness of protected areas for bird conservation depends on guild*. *Diversity and Distributions* **24**, 1083–1091. https://doi.org/10.1111/ddi.12756.

Eftekhari A, Pasadakis D, Bollhöfer M, Scheidegger S, Schenk O (2021). *Block-enhanced precision matrix estimation for large-scale datasets*. *Journal of Computational Science* **53**. https://doi.org/10.1016/j.jocs.2021.101389.

Escamilla Molgora JM, Sedda L, Diggle P, Atkinson PM (2022). *A joint distribution framework to improve presence-only species distribution models by exploiting opportunistic surveys*. *Journal of Biogeography* **49**, 1176–1192. https://doi.org/10.1111/jbi.14365.

Farr MT, Green DS, Holekamp KE, Zipkin EF (2021). *Integrating distance sampling and presence-only data to estimate species abundance*. *Ecology* **102**, e03204. https://doi.org/10.1002/ecy.3204.

Fawcett T (2006). *An introduction to ROC analysis*. *Pattern Recognition Letters* **27**, 861–874. https://doi.org/10.1016/j.patrec.2005.10.010.

643 Fick SE, Hijmans RJ (2017). *WorldClim 2: new 1-km spatial resolution climate surfaces for global*
644 *land areas*. *International Journal of Climatology* **37**, 4302–4315. https://doi.org/10.1002/
645 joc.5086.
646 Fithian W, Elith J, Hastie T, Keith DA (2015). *Bias correction in species distribution models: pooling*
647 *survey and collection data for multiple species*. *Methods in Ecology and Evolution* **6**, 424–438.
648 https://doi.org/10.1111/2041-210X.12242.
649 Fithian W, Hastie T (2013). *Finite-sample equivalence in statistical models for presence-only data*.
650 *The Annals of Applied Statistics* **7**, 1917–1939. https://doi.org/10.1214/13-AOAS667.
651 Flousek J, Telenský T, Hanzelka J, Reif J (2015). *Population Trends of Central European Montane*
652 *Birds Provide Evidence for Adverse Impacts of Climate Change on High-Altitude Species*. *PLOS*
653 *ONE* **10**, e0139465. https://doi.org/10.1371/journal.pone.0139465.
654 Fontaine B, Moussy C, Chiffard Carricaburu J, Dupuis J, Schmaltz L, Lorrillière R, Loïs G, Gau-
655 dard C, Couzi L (2020). *Suivi des oiseaux communs en France 1989-2019 : 30 ans de suivis*
656 *participatifs*. MNHN- Centre d'Ecologie et des Sciences de la Conservation, LPO BirdLife
657 France - Service Connaissance, Ministère de la Transition écologique et solidaire., p. 46.
658 URL: https://www.vigienature.fr/sites/vigienature/files/atoms/files/
659 syntheseoiseauxcommuns2020_final.pdf.
660 El-Gabbas A, Dormann CF (2018). *Improved species-occurrence predictions in data-poor regions:*
661 *using large-scale data and bias correction with down-weighted Poisson regression and Maxent*.
662 *Ecography* **41**, 1161–1172. https://doi.org/10.1111/ecog.03149.
663 Gaedke-Merzhäuser L, Niekerk J, Schenk O, Rue H (2023). *Parallelized integrated nested Laplace*
664 *approximations for fast Bayesian inference*. *Statistics and Computing* **33**, 25. https://doi.org/
665 10.1007/s11222-022-10192-1.
666 Gilks WR, Richardson S, Spiegelhalter D (1995). *Markov Chain Monte Carlo in Practice*. New York,
667 NY: Chapman and Hall/CRC. 512 pp. https://doi.org/10.1201/b14835.
668 Giraud C, Calenge C, Coron C, Julliard R (2016). *Capitalizing on opportunistic data for monitoring*
669 *relative abundances of species*. *Biometrics* **72**, 649–658. https://doi.org/10.1111/biom.
670 12431.
671 Gregory RD, Skorpilova J, Vorisek P, Butler S (2019). *An analysis of trends, uncertainty and species*
672 *selection shows contrasting trends of widespread forest and farmland birds in Europe*. *Ecological*
673 *Indicators* **103**, 676–687. https://doi.org/10.1016/j.ecolind.2019.04.064.
674 Gregory RD, Vorisek P, Van Strien A, Gmelig Meyling AW, Jiguet F, Fornasari L, Reif J, Chylarecki
675 P, Burfield IJ (2007). *Population trends of widespread woodland birds in Europe*. *Ibis* **149** (s2),
676 78–97. https://doi.org/10.1111/j.1474-919X.2007.00698.x.
677 Harris I, Osborn TJ, Jones P, Lister D (2020). *Version 4 of the CRU TS monthly high-resolution*
678 *gridded multivariate climate dataset*. *Scientific Data* **7**, 109. https://doi.org/10.1038/
679 s41597-020-0453-3.
680 Haupert S, Sèbe F, Sueur J (2023). *Physics-based model to predict the acoustic detection distance*
681 *of terrestrial autonomous recording units over the diel cycle and across seasons: Insights from an*
682 *Alpine and a Neotropical forest*. *Methods in Ecology and Evolution* **14**, 614–630. https://doi.
683 org/10.1111/2041-210X.14020.
684 Heldbjerg H, Sunde P, Fox AD (2018). *Continuous population declines for specialist farmland birds*
685 *1987-2014 in Denmark indicates no halt in biodiversity loss in agricultural habitats*. *Bird Conser-*
686 *vation International* **28**, 278–292. https://doi.org/10.1017/S0959270916000654.

687 Henckel L, Bradter U, Jönsson M, Isaac NJB, Snäll T (2020). *Assessing the usefulness of citizen*
688 *science data for habitat suitability modelling: Opportunistic reporting versus sampling based on a*
689 *systematic protocol*. *Diversity and Distributions* **26**, 1276–1290. https://doi.org/10.1111/
690 ddi.13128.
691 Hijmans RJ (2024). *terra: Spatial Data Analysis*. R package version 1.7-71. URL: https://CRAN.R-
692 project.org/package=terra.
693 Horns JJ, Adler FR, Şekercioğlu ÇH (2018). *Using opportunistic citizen science data to estimate*
694 *avian population trends*. *Biological Conservation* **221**, 151–159. https://doi.org/10.1016/
695 j.biocon.2018.02.027.
696 IGN (2018). *RGE ALTI® [Data set]*. URL: https://geoservices.ign.fr/rgealti.
697 Illian JB, Martino S, Sørbye SH, Gallego-Fernández JB, Zunzunegui M, Esquivias MP, Travis JMJ
698 (2013). *Fitting complex ecological point process models with integrated nested Laplace approxi-*
699 *mation*. *Methods in Ecology and Evolution* **4**, 305–315. https://doi.org/10.1111/2041-
700 210x.12017.
701 Inger R, Gregory R, Duffy JP, Stott I, Voříšek P, Gaston KJ (2015). *Common European birds are de-*
702 *clining rapidly while less abundant species' numbers are rising*. *Ecology Letters* **18**, 28–36. https:
703 //doi.org/10.1111/ele.12387.
704 Inglada J, Vincent A, Thierion V (2018). *Theia OSO Land Cover Map 2018 [Data set]*. https://
705 doi.org/10.5281/zenodo.3613415.
706 IPBES (2019). *Summary for policymakers of the global assessment report on biodiversity and ecosys-*
707 *tem services of the Intergovernmental Science-Policy Platform on Biodiversity and Ecosystem Ser-*
708 *vices*. Bonn, Germany. 56 pages. URL: https://doi.org/10.5281/zenodo.3553579.
709 Janžekovič F, Novak T (2012). *PCA – A Powerful Method for Analyze Ecological Niches*. In: *Principal*
710 *Component Analysis*. 8. Rijeka: IntechOpen. https://doi.org/10.5772/38538.
711 Jiguet F, Devictor V, Julliard R, Couvet D (2012). *French citizens monitoring ordinary birds provide*
712 *tools for conservation and ecological sciences*. *Acta Oecologica* **44**, 58–66. https://doi.org/
713 10.1016/j.actao.2011.05.003.
714 Jin Huang, Ling C (2005). *Using AUC and accuracy in evaluating learning algorithms*. *IEEE Transac-*
715 *tions on Knowledge and Data Engineering* **17**, 299–310. https://doi.org/10.1109/TKDE.
716 2005.50.
717 Jung Y (2018). *Multiple predicting K -fold cross-validation for model selection*. *Journal of Nonpara-*
718 *metric Statistics* **30**, 197–215. https://doi.org/10.1080/10485252.2017.1404598.
719 Kamp J, Frank C, Trautmann S, Busch M, Dröschmeister R, Flade M, Gerlach B, Karthäuser J,
720 Kunz F, Mitschke A, Schwarz J, Sudfeldt C (2021). *Population trends of common breeding birds*
721 *in Germany 1990–2018*. *Journal of Ornithology* **162**, 1–15. https://doi.org/10.1007/
722 s10336-020-01830-4.
723 Kervellec M, Milleret C, Vanpé C, Quenette PY, Sentilles J, Palazón S, Jordana IA, Jato R, Elósegui
724 Irurtia MM, Gimenez O (2023). *Integrating opportunistic and structured non-invasive surveys*
725 *with spatial capture-recapture models to map connectivity of the Pyrenean brown bear population*.
726 *Biological Conservation* **278**, 109875. https://doi.org/10.1016/j.biocon.2022.109875.
727 Kéry M, Royle JA, Schmid H, Schaub M, Volet B, Häfliger G, Zbinden N (2010). *Site-occupancy*
728 *distribution modeling to correct population-trend estimates derived from opportunistic observa-*
729 *tions*. *Conservation Biology* **24**, 1388–1397. https://doi.org/10.1111/j.1523-1739.2010.
730 01479.x.

Knape J (2016). *Decomposing trends in Swedish bird populations using generalized additive mixed models*. *Journal of Applied Ecology* **53**, 1852–1861. https://doi.org/10.1111/1365-2664.12720.

Lehikoinen A, Brotons L, Calladine J, Campedelli T, Escandell V, Flousek J, Grueneberg C, Haas F, Harris S, Herrando S, Husby M, Jiguet F, Kålås JA, Lindström Å, Lorrillière R, Molina B, Pladevall C, Calvi G, Sattler T, Schmid H, et al. (2019). *Declining population trends of European mountain birds*. *Global Change Biology* **25**, 577–588. https://doi.org/10.1111/gcb.14522.

Lindgren F, Rue H, Lindström J (2011). *An explicit link between Gaussian fields and Gaussian Markov random fields: the stochastic partial differential equation approach*. *Journal of the Royal Statistical Society Series B: Statistical Methodology* **73**, 423–498. https://doi.org/10.1111/j.1467-9868.2011.00777.x.

Link WA, Cam E, Nichols JD, Cooch EG (2002). *Of Bugs and Birds: Markov Chain Monte Carlo for Hierarchical Modeling in Wildlife Research*. *The Journal of Wildlife Management* **66**, 277. https://doi.org/10.2307/3803160.

McVicar TR, Körner C (2013). *On the use of elevation, altitude, and height in the ecological and climatological literature*. *Oecologia* **171**, 335–337. https://doi.org/10.1007/s00442-012-2416-7.

Moreira GA, Menezes R, Wise L (2024). *Presence-Only for Marked Point Process Under Preferential Sampling*. *Journal of Agricultural, Biological and Environmental Statistics* **29**, 92–109. https://doi.org/10.1007/s13253-023-00558-x.

Murtagh F, Legendre P (2014). *Ward's Hierarchical Agglomerative Clustering Method: Which Algorithms Implement Ward's Criterion? Journal of Classification* **31**, 274–295. https://doi.org/10.1007/s00357-014-9161-z.

Newton I (2004). *The recent declines of farmland bird populations in Britain: an appraisal of causal factors and conservation actions*. *Ibis* **146**, 579–600. https://doi.org/10.1111/j.1474-919X.2004.00375.x.

Noël F, Combrisson D, Geoffroy JJ, Nicolas MG (2023). *Synthèse des connaissances sur les Isopodes et Diplopodes terrestres du Parc national des Écrins (SE France)*. *Naturae*, 151–170. https://doi.org/10.5852/naturae2023a9.

Palacín C, Alonso JC (2018). *Failure of EU Biodiversity Strategy in Mediterranean farmland protected areas*. *Journal for Nature Conservation* **42**, 62–66. https://doi.org/10.1016/j.jnc.2018.02.008.

Pasadakis D, Bollhöfer M, Schenk O (2023). *Sparse Quadratic Approximation for Graph Learning*. *IEEE Transactions on Pattern Analysis and Machine Intelligence* **45**, 11256–11269. https://doi.org/10.1109/TPAMI.2023.3263969.

Pedersen EJ, Miller DL, Simpson GL, Ross N (2019). *Hierarchical generalized additive models in ecology: an introduction with mgcv*. *PeerJ* **7**, e6876. https://doi.org/10.7717/peerj.6876.

Phillips SJ, Anderson RP, Schapire RE (2006). *Maximum entropy modeling of species geographic distributions*. *Ecological Modelling* **190**, 231–259. https://doi.org/10.1016/j.ecolmodel.2005.03.026.

Phillips SJ, Dudík M, Elith J, Graham CH, Lehmann A, Leathwick J, Ferrier S (2009). *Sample selection bias and presence-only distribution models: implications for background and pseudo-absence data*. *Ecological Applications* **19**, 181–197. https://doi.org/10.1890/07-2153.1.

R Core Team (2024). *R: A Language and Environment for Statistical Computing*. R Foundation for Statistical Computing. Vienna, Austria. URL: https://www.r-project.org.

Ramsay JO, Silverman BW (2005). *Functional Data Analysis*. Springer Series in Statistics. New York, NY: Springer. https://doi.org/10.1007/b98888.

Ramsay J, Hooker G, Graves S (2009). *Functional Data Analysis with R and MATLAB*. New York, NY: Springer. https://doi.org/10.1007/978-0-387-98185-7.

Reif J, Storch D, Voříšek P, Šťastný K, Bejček V (2008a). *Bird-habitat associations predict population trends in central European forest and farmland birds*. *Biodiversity and Conservation* **17**, 3307–3319. https://doi.org/10.1007/s10531-008-9430-4.

Reif J, Voříšek P, Š?astný K, Bejček V, Petr J (2008b). *Agricultural intensification and farmland birds: new insights from a central European country*. *Ibis* **150**, 596–605. https://doi.org/10.1111/j.1474-919X.2008.00829.x.

Renner IW, Elith J, Baddeley A, Fithian W, Hastie T, Phillips SJ, Popovic G, Warton DI (2015). *Point process models for presence-only analysis*. *Methods in Ecology and Evolution* **6**, 366–379. https://doi.org/10.1111/2041-210X.12352.

Renner IW, Warton DI (2013). *Equivalence of MAXENT and Poisson Point Process Models for Species Distribution Modeling in Ecology*. *Biometrics* **69**, 274–281. https://doi.org/10.1111/j.1541-0420.2012.01824.x.

Rigal S, Dakos V, Alonso H, Auniņš A, Benkő Z, Brotons L, Chodkiewicz T, Chylarecki P, Carli E, Moral JC, Domşa C, Escandell V, Fontaine B, Foppen R, Gregory R, Harris S, Herrando S, Husby M, Ieronymidou C, Jiguet F, et al. (2023). *Farmland practices are driving bird population decline across Europe*. *Proceedings of the National Academy of Sciences* **120**, e2216573120. https://doi.org/10.1073/pnas.2216573120.

Rue H, Martino S, Chopin N (2009). *Approximate Bayesian inference for latent Gaussian models by using integrated nested Laplace approximations*. *Journal of the Royal Statistical Society Series B: Statistical Methodology* **71**, 319–392. https://doi.org/10.1111/j.1467-9868.2008.00700.x.

Sanderson FJ, Kucharz M, Jobda M, Donald PF (2013). *Impacts of agricultural intensification and abandonment on farmland birds in Poland following EU accession*. *Agriculture, Ecosystems & Environment* **168**, 16–24. https://doi.org/10.1016/j.agee.2013.01.015.

Schulze ED, Craven D, Durso AM, Reif J, Guderle M, Kroiher F, Hennig P, Weiserbs A, Schall P, Ammer C, Eisenhauer N (2019). *Positive association between forest management, environmental change, and forest bird abundance*. *Forest Ecosystems* **6**, 3. https://doi.org/10.1186/s40663-019-0160-8.

Silva JP, Correia R, Alonso H, Martins RC, D'Amico M, Delgado A, Sampaio H, Godinho C, Moreira F (2018). *EU protected area network did not prevent a country wide population decline in a threatened grassland bird*. *PeerJ* **6**, e4284. https://doi.org/10.7717/peerj.4284.

Snäll T, Kindvall O, Nilsson J, Pärt T (2011). *Evaluating citizen-based presence data for bird monitoring*. *Biological Conservation* **144**, 804–810. https://doi.org/10.1016/j.biocon.2010.11.010.

Soriano-Redondo A, Jones-Todd CM, Bearhop S, Hilton GM, Lock L, Stanbury A, Votier SC, Illian JB (2019). *Understanding species distribution in dynamic populations: a new approach using spatio-temporal point process models*. *Ecography* **42**, 1092–1102. https://doi.org/10.1111/ecog.03771.

Timmers R, Kuijk M, Verweij PA, Ghazoul J, Hautier Y, Laurance WF, Arriaga-Weiss SL, Askins RA, Battisti C, Berg Å, Daily GC, Estades CF, Frank B, Kurosawa R, Pojar RA, Woinarski JC, Soons MB (2022). *Conservation of birds in fragmented landscapes requires protected areas*. *Frontiers in Ecology and the Environment* **20**, 361–369. https://doi.org/10.1002/fee.2485.

Traba J, Morales MB (2019). *The decline of farmland birds in Spain is strongly associated to the loss of fallowland*. *Scientific Reports* **9**, 9473. https://doi.org/10.1038/s41598-019-45854-0.

Valavi R, Guillera-Arroita G, Lahoz-Monfort JJ, Elith J (2022). *Predictive performance of presence-only species distribution models: a benchmark study with reproducible code*. *Ecological Monographs* **92**, e01486. https://doi.org/10.1002/ecm.1486.

Van Strien AJ, Van Swaay CA, Termaat T (2013). *Opportunistic citizen science data of animal species produce reliable estimates of distribution trends if analysed with occupancy models*. *Journal of Applied Ecology* **50**, 1450–1458. https://doi.org/10.1111/1365-2664.12158.

Ver Hoef JM, Johnson D, Angliss R, Higham M (2021). *Species density models from opportunistic citizen science data*. *Methods in Ecology and Evolution* **12**, 1911–1925. https://doi.org/10.1111/2041-210X.13679.

Warton DI, Renner IW, Ramp D (2013). *Model-Based Control of Observer Bias for the Analysis of Presence-Only Data in Ecology*. *PLoS ONE* **8**, e79168. https://doi.org/10.1371/journal.pone.0079168.

Warton DI, Shepherd LC (2010). *Poisson point process models solve the "pseudo-absence problem" for presence-only data in ecology*. *The Annals of Applied Statistics* **4**. https://doi.org/10.1214/10-AOAS331.

Wikle CK (2003). *Hierarchical Bayesian Models for Predicting the Spread of Ecological Processes*. *Ecology* **84**, 1382–1394. https://doi.org/10.1890/0012-9658(2003)084[1382:HBMFPT]2.0.CO;2.

Wretenberg J, Lindström Å, Svensson S, Thierfelder T, Pärt T (2006). *Population trends of farmland birds in Sweden and England: similar trends but different patterns of agricultural intensification*. *Journal of Applied Ecology* **43**, 1110–1120. https://doi.org/10.1111/j.1365-2664.2006.01216.x.

Zamora R, Barea-Azcón JM (2015). *Long-Term Changes in Mountain Passerine Bird Communities in the Sierra Nevada (Southern Spain): A 30-Year Case Study*. *Ardeola* **62**, 3–18. https://doi.org/10.13157/arla.62.1.2015.3.

849

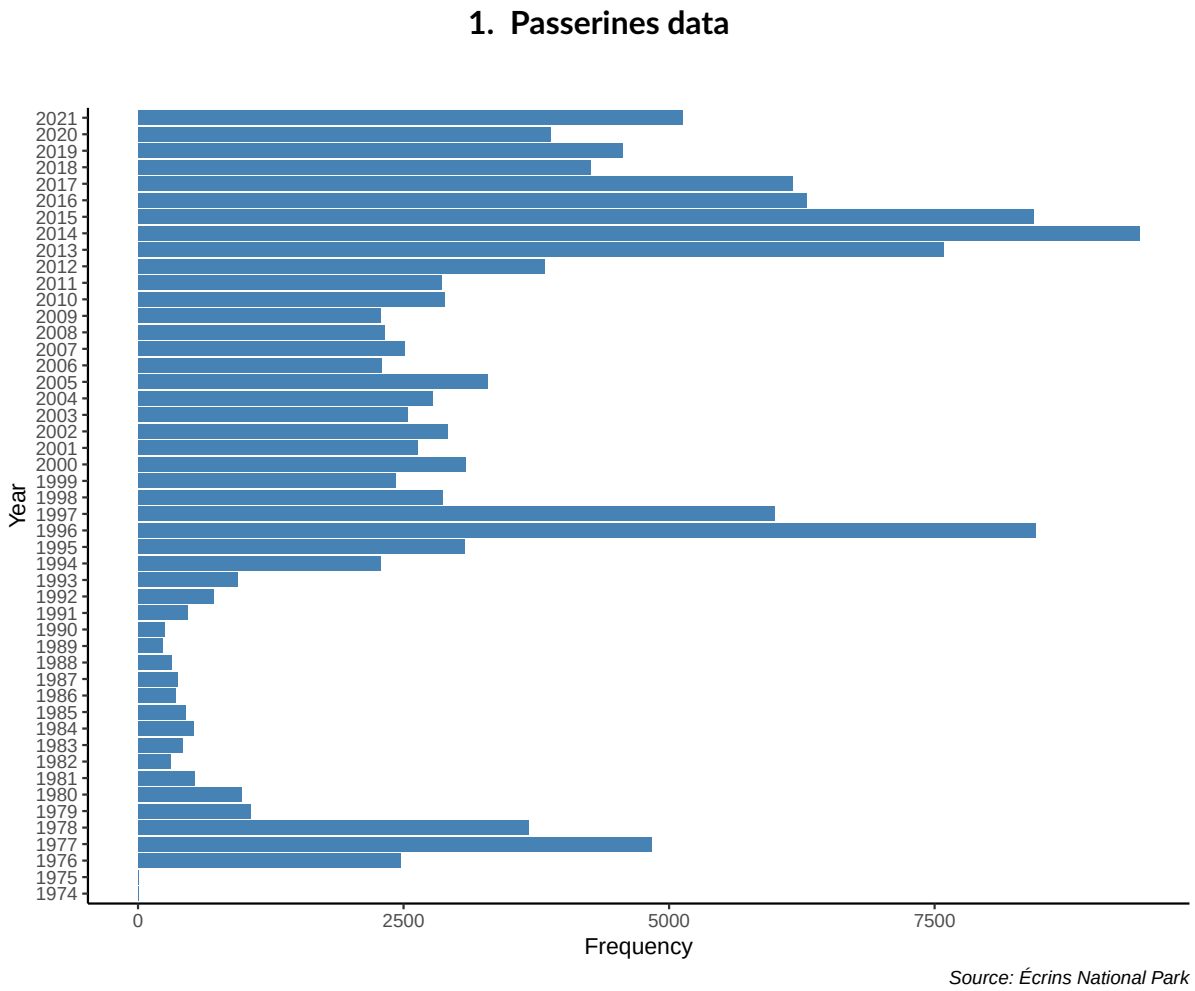

Figure 6 – Number of reported opportunistic passerine occurrences in the Écrins National Park between 1974 and 2021. Three passerines were excluded from the barplot: Common Raven (*Corvus corax*), Red-billed Chough (*Pyrrhocorax pyrrhocorax*), Alpine Chough (Pyrrhocorax graculus) for a total of 102,513 occurrences.

2. OSO covariates

The OSO data are raster data produced at 10m and 20m spatial resolution. These two outputs are provided because the Sentinel-2 spectral bands used in the production process are acquired at 10m (visible and near-infrared) and 20m (red-edge, near and medium infrared) (Inglada, 2018). The nomenclature includes 24 classes. We then apply the nearest neighbor strategy to adjust the values to a 5m resolution, aligning with the elevation data resolution used in this study (IGN, 2018). We present in Table 1 the percentage of coverage for each OSO class in the Écrins National Park. The percentage of coverage for a chosen class is computed as the number of spatial cells of this class over the total number of spatial cells, based on a 5m regular grid of the Écrins National Park domain.

Table 1 – OSO data nomenclature including percentage coverage at a 5m resolution Écrins National Park. Classes with a percentage of coverage greater than 1% are in bold for easier readability.

Number	Nomenclature	Percentage
1	Dense buildings	<0.1%
2	Sparse buildings	0.6%
3	Industrial and commercial areas	0.3%
4	Road surfaces	<0.1%
5	Rapeseed	<0.1%
6	Cereal with straw	0.1%
7	Protein crops	<0.1%
8	Soybean	<0.1%
9	Sunflower	<0.1%
10	Corn	0.1%
11	Rice	<0.1%
12	Tubers/roots	<0.1%
13	**Meadows**	**2.1%**
14	Orchards	<0.1%
15	Vineyards	<0.1%
16	**Deciduous forests**	**3.7%**
17	**Coniferous forests**	**16.0%**
18	**Grasslands**	**40.1%**
19	**Woody heaths**	**5.3%**
20	**Mineral surfaces**	**27.7%**
21	Beaches and dunes	0.1%
22	**Glaciers or snow**	**2.8%**
23	**Water**	**1.1%**
0	Other	<0.1%

Some classes are nearly absent in the Écrins National Park. Hence, the first four classes: *Dense buildings*, *Sparse buildings*, *Industrial and commercial areas* and *Road surfaces* are gathered into the **Urban** terminology. The following classes: *Rapeseed*, *Cereal with straw*, *Legumes*, *Soybean*, *Sunflower*, *Corn*, *Rice*, *Tubers/roots*, *Orchards*, *Vineyards* are gathered into the **Crops** terminology. Due to their very low percentage of surface area, the classes *Beaches and dunes* and *Other* are excluded from the analysis.

Hence, the land cover land used classification used in the article is composed of 10 classes and is summarized in Table 2.

Table 2 – OSO data nomenclature adjusted for the Écrins National Park, including percentage coverage at a 5m resolution in the Écrins National Park.

Nomenclature	Percentage
Urban	0.9%
Crops	0.3%
Meadows	2.1%
Deciduous forests	3.7%
Coniferous forests	16.0%
Grasslands	40.1%
Woody heaths	5.3%
Mineral surfaces	27.7%
Glaciers or snow	2.8%
Water	1.1%

Using a spatial grid with a resolution of 500m, we calculated the coverage percentage of these 10 classes in each spatial cell to construct the OSO covariates, which formed the basis of the Principal Component Analysis.

References

Inglada, J, Vincent, A, & Thierion, V (2018). Theia OSO Land Cover Map 2018 [Data set]. Zenodo. https://doi.org/10.5281/zenodo.3613415

IGN (2018). *RGE ALTI*®. Version 2.0.

875

3. PCA figures

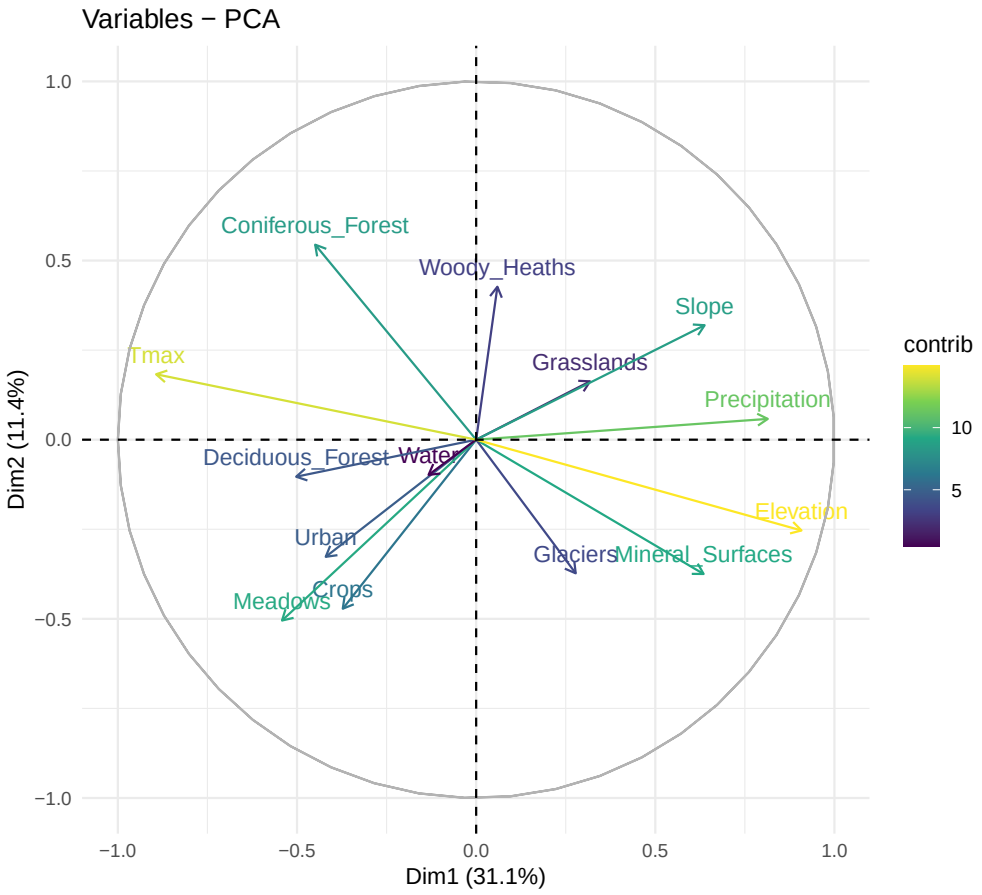

Figure 7 – Correlation circles of axis 1 and 2 of the PCA.

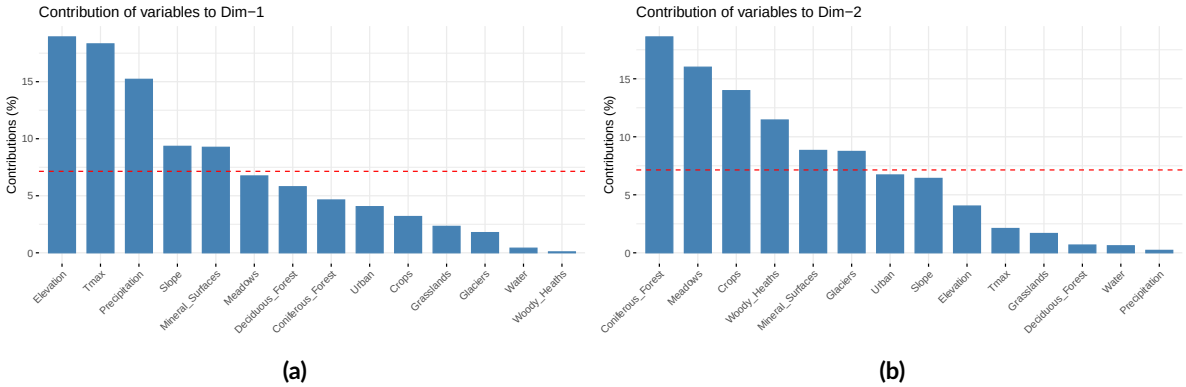

Figure 8 – Contribution of each spatial covariate to the axis 1 (a) and 2 (b) of the PCA.

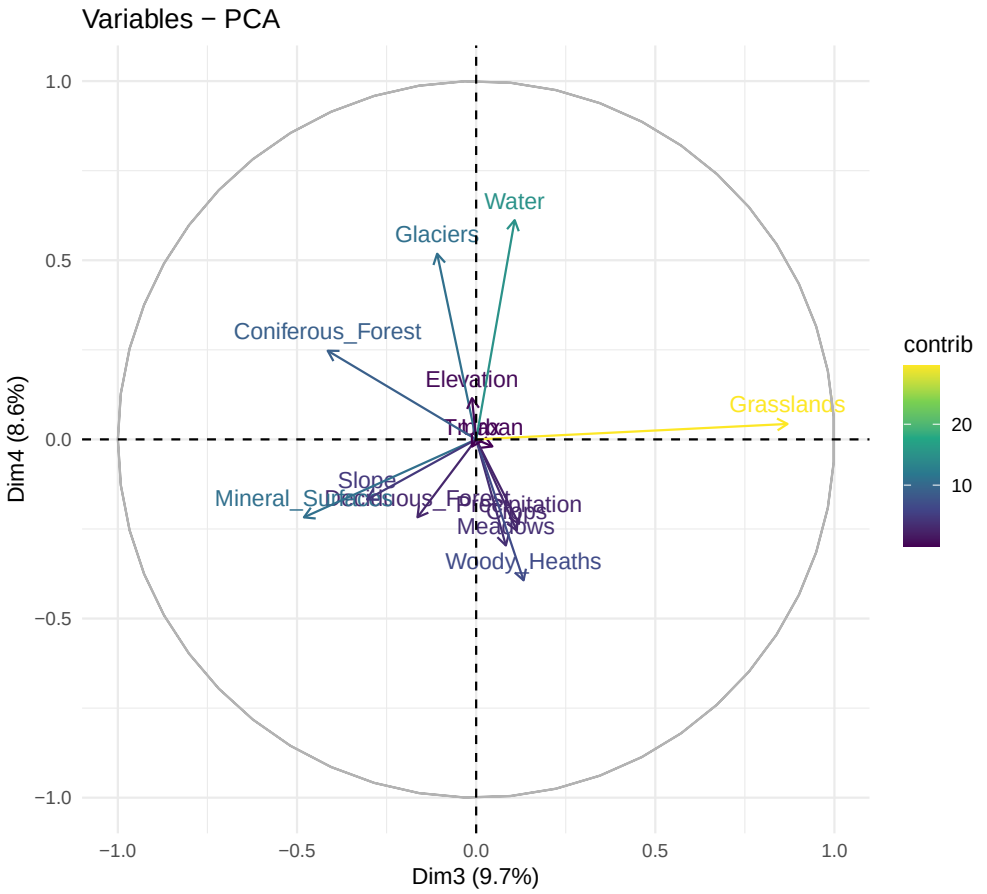

Figure 9 – Correlation circles of axis 3 and 4 of the PCA.

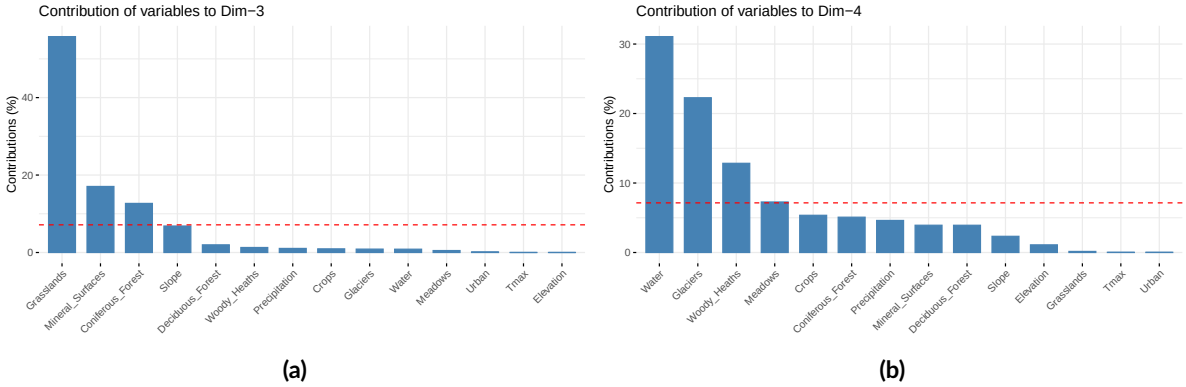

Figure 10 – Contribution of each spatial covariate to the axis 3 (a) and 4 (b) of the PCA.

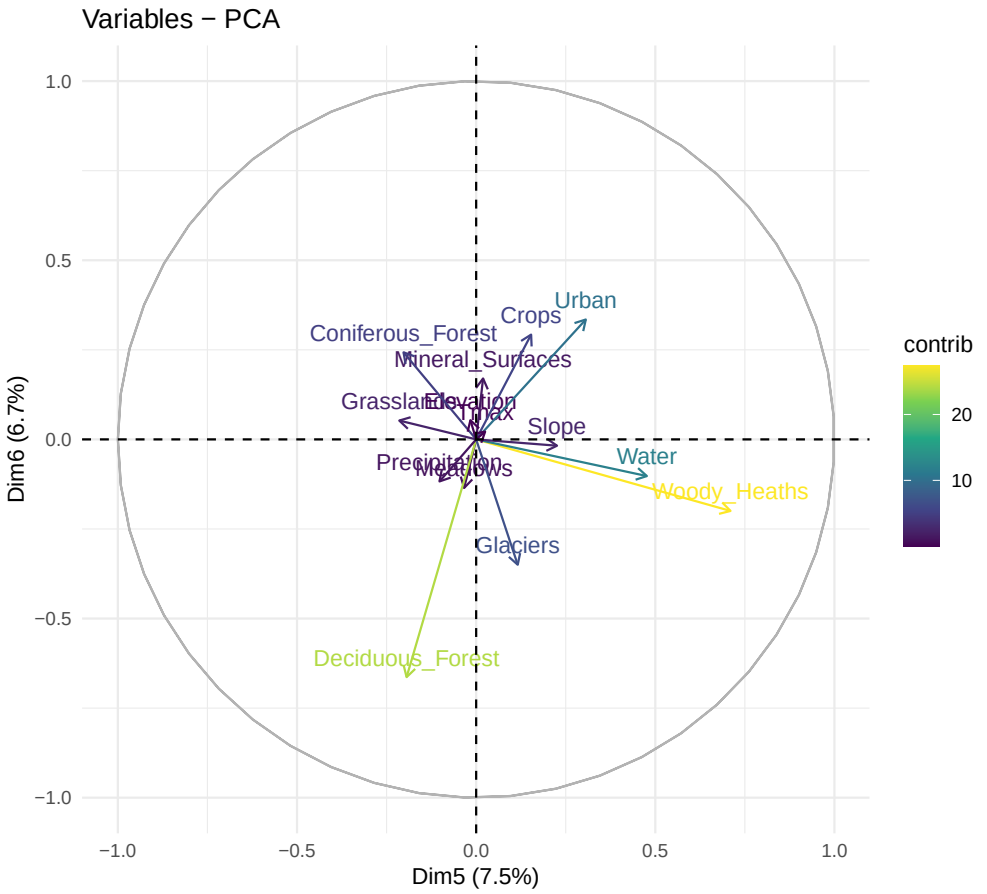

Figure 11 – Correlation circles of axis 5 and 6 of the PCA.

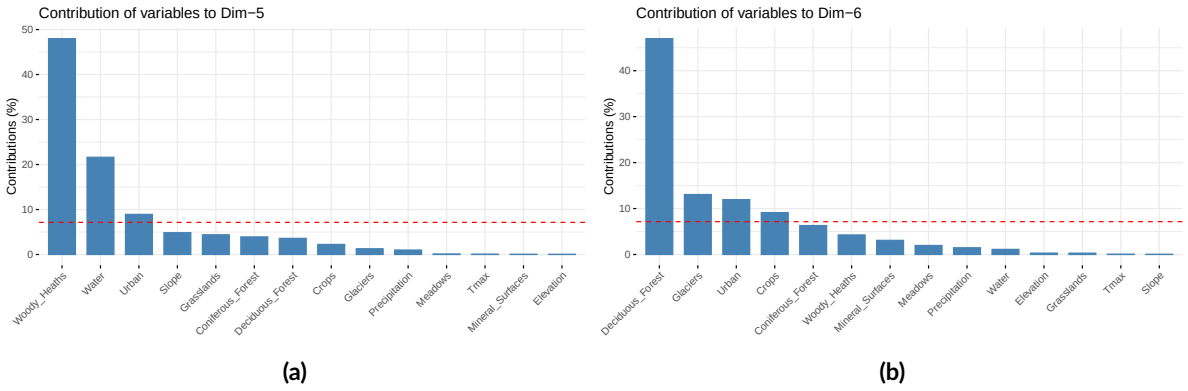

Figure 12 – Contribution of each spatial covariate to the axis 5 (a) and 6 (b) of the PCA.

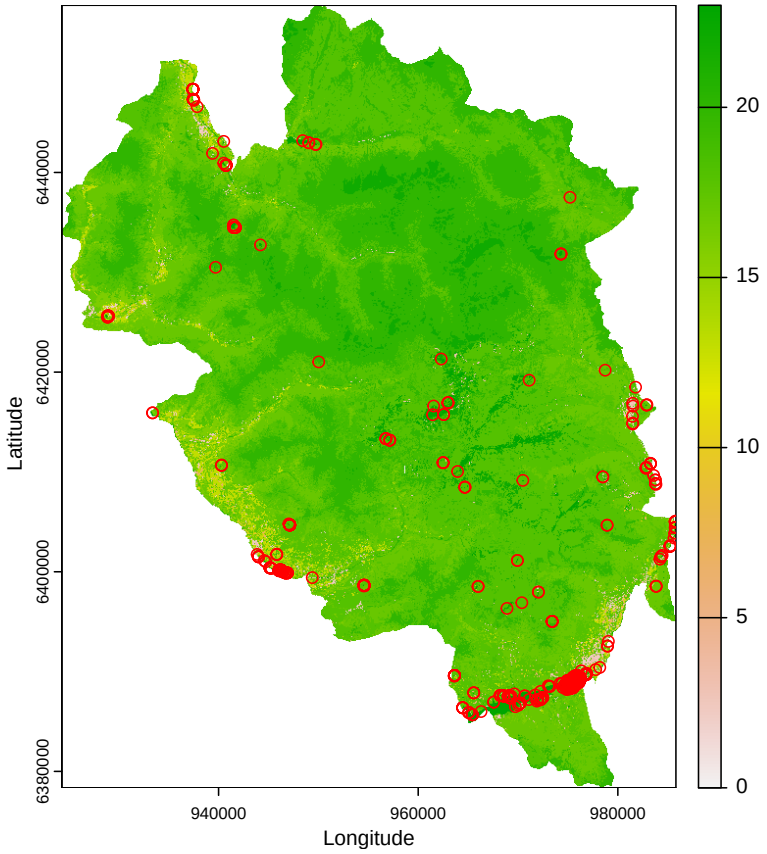

Figure 13 – Map of passerine occurrences in wetlands (red circles) on OSO land cover land used classification in the Écrins National Park . Each number correspond to a class described in Table 1. The observations mainly occur in urban wetlands in the valleys.

4. Parameter models – Priors

We will now describe each prior used, i.e., the structure of the model components before updating them with information from observation data to obtain their posterior distributions. Each of the parameters β_i or γ_i associated with the fixed covariate effects has a very weakly informative Gaussian prior distribution centered at zero and with a precision hyperparameter $\tau_\beta = 10^{-3}$. For each month m, the spatial field $W_i^{(m)}$ is *a priori* represented using a 2-dimensional Gaussian random field based on the SPDE approach, where the Matérn covariance function has a fixed shape parameter $\nu^{(m)} = 1$, while the effective range, $\rho_i^{(m)}$, and the standard deviation, $\sigma_i^{(m)}$, are endowed with so-called penalized complexity priors (PC priors, Simpson et al., 2017): *a priori*, the probability of having range less than $\rho_0^{(m)} = 1$ is set to $\alpha_\rho^{(m)} = 0.5$, and the probability of having standard deviation larger than $\sigma_0^{(m)} = 1$ is set to $\alpha_\sigma^{(m)} = 0.5$. Since the spatial field $W_i^{(m)}$ is replicated month by month, a cyclic $AR(1)$ correlation structure (Box et al., 2015) is applied such that the value of $W_i^{(m)}$ is informed by the values of $W_i^{(m-1)}$ and $W_i^{(m+1)}$, where $m-1 = 12$ for $m = 1$ and $m+1 = 1$ for $m = 12$. Regarding each period p, the inter-annual random effects $f_i(p)$ have independent and identically distributed Gaussian prior distributions with a precision hyperparameter $\tau_f = 10^{-3}$.

References

Box G.E.P., Gwilym M.J., Reinsel G.C., Ljung G.M. (2015). Time Series Analysis : Forecasting and Control. 5th edition. Hoboken, New Jersey: John Wiley and Sons Inc. 712 pp.

Simpson D., Rue H., Riebler A., Martins T.G., Sørbye S.H. (2017). Penalising Model Component Complexity: A Principled, Practical Approach to Constructing Priors. Statistical Science 32, 1–28. https://doi.org/10.1214/16-STS576.

898

5. Temporal and spatial cross-validation scenarios

Table 3 – Table of temporal cross-validation scenarios. The total number of space-time cells with at least one occurrence in the target-group is 32,486. For each scenario, half of these cells of the corresponding period of four years and their associated occurrences are removed.

Scenario	Period	Removed cells	Percentage
13	1994-1997	1782	5.5%
14	1998-2001	1274	3.9%
15	2002-2005	1512	4.7%
16	2006-2009	1525	4.7%
17	2010-2013	2670	8.2%
18	2014-2017	4477	13.8%
19	2018-2021	3001	9.2%

Table 4 – Table of spatial cross-validation scenarios. The total number of space-time cells with at least one occurrence in the target-group is 32,486. For each scenario, the cells of a given city and their associated occurrences are removed.

Scenario	Period	Removed cells	Percentage
20	Saint-Christophe-en-Oisans	4407	13.6%
21	Valjouffrey	2473	7.6%
22	La Chapelle-en-Valgaudémar	2700	8.3%
23	Orcières	2167	6.7%
24	Châteauroux-les-Alpes	1839	5.7%
25	L'Argentiére-la-Bessée	1345	4.1%
26	La Grave	2656	8.2%

899

6. Habitat preferences

Table 5 – Mean estimated parameters on spatial covariates : PCA Axis 1 to 3. Significant parameters based on the 95% interval of credibility are in bold.

Species (Occurrences)	High Elevation	Coniferous forests	Grasslands
Acanthis flammea (464)	0.03	0.1	**0.39**
Acrocephalus palustris (138)	**-0.39**	0.25	**0.45**
Aegithalos caudatus (1599)	**-0.29**	**0.15**	**-0.29**
Alauda arvensis (1068)	**0.98**	**-0.54**	**0.73**
Anthus spinoletta (1934)	**1**	**-0.57**	**0.65**
Anthus trivialis (1292)	**-0.13**	**0.53**	**0.47**
Bombycilla garrulus (146)	NA	NA	NA
Carduelis carduelis (1549)	**-0.21**	**-0.12**	**0.24**
Carduelis citrinella (730)	**0.49**	0.04	**0.33**
Certhia brachydactyla (449)	**-0.62**	0.07	**-0.35**
Certhia familiaris (984)	-0.09	**0.71**	**-0.27**
Chloris chloris (668)	**-0.36**	**-0.4**	-0.11
Cinclus cinclus (1887)	**-0.67**	**0.11**	-0.05
Coccothraustes coccothraustes (486)	**-0.18**	-0.18	-0.11
Corvus corone (1745)	**-0.21**	-0.04	**0.24**
Corvus corone cornix (187)	**-0.66**	0.08	**1.02**
Corvus monedula (152)	-0.43	-0.05	-0.71
Cyanistes caeruleus (1892)	**-0.27**	0.01	**-0.17**
Delichon urbicum (734)	**0.21**	**-0.13**	-0.04
Emberiza cia (1548)	**0.1**	0.01	0.05
Emberiza cirlus (202)	**-0.69**	0.16	0.11
Emberiza citrinella (1734)	**-0.21**	-0.07	**0.39**
Emberiza hortulana (134)	0.02	0.24	**0.91**
Erithacus rubecula (3354)	**-0.35**	**0.26**	**-0.18**
Ficedula hypoleuca (273)	**-0.55**	0.13	0.05
Fringilla coelebs (5447)	**-0.26**	**0.3**	0.03
Fringilla montifringilla (551)	**-0.22**	-0.01	0.04
Garrulus glandarius (2201)	**-0.37**	**0.31**	**-0.13**
Hirundo rustica (642)	**-0.38**	-0.11	**0.38**
Lanius collurio (834)	**-0.24**	-0.14	**0.35**
Linaria cannabina (1369)	**0.47**	**-0.31**	**0.55**
Lophophanes cristatus (2160)	**-0.16**	**0.63**	**-0.17**
Loxia curvirostra (1890)	**0.22**	**0.83**	**0.34**
Lullula arborea (321)	-0.15	**0.48**	**0.94**
Luscinia megarhynchos (376)	**-0.46**	0.12	0.29
Monticola saxatilis (566)	**1.16**	**-0.35**	**0.47**
Montifringilla nivalis (999)	**1.48**	**-1.13**	**0.44**
Motacilla alba (1088)	**-0.55**	**-0.22**	**0.22**
Motacilla cinerea (697)	**-0.37**	-0.05	-0.08

Motacilla flava (144)	-0.24	**-0.59**	**0.37**
Nucifraga caryocatactes (2275)	**0.39**	**0.49**	0.02
Oenanthe oenanthe (2263)	**0.94**	**-0.68**	**0.66**
Parus major (3165)	**-0.31**	0	**-0.16**
Passer domesticus (947)	**-0.45**	**-0.44**	-0.09
Passer montanus (209)	**-0.9**	0.22	**0.8**
Periparus ater (3595)	**-0.18**	**0.45**	**-0.21**
Petronia petronia (197)	**-0.48**	**-0.42**	0.24
Phoenicurus ochruros (4183)	**0.48**	**-0.43**	**0.11**
Phoenicurus phoenicurus (668)	**-0.27**	**-0.24**	0.07
Phylloscopus bonelli (1668)	**-0.17**	**0.17**	**-0.28**
Phylloscopus collybita (2944)	**-0.27**	**0.3**	-0.03
Pica pica (1061)	**-0.32**	**-0.18**	**0.24**
Poecile montanus (2433)	0.07	**0.7**	-0.01
Poecile palustris (774)	**-0.35**	0.09	**-0.21**
Prunella collaris (1775)	**1.2**	**-0.78**	0.05
Prunella modularis (1386)	**0.2**	**0.29**	**0.24**
Ptyonoprogne rupestris (1695)	**0.26**	**-0.11**	**-0.12**
Pyrrhula pyrrhula (1816)	**-0.32**	**0.44**	**-0.29**
Regulus ignicapilla (686)	**-0.37**	**0.74**	**-0.33**
Regulus regulus (1030)	**-0.27**	**0.79**	**-0.22**
Saxicola rubetra (944)	**-0.2**	**-0.15**	**0.74**
Saxicola rubicola (313)	-0.14	-0.13	**0.75**
Serinus serinus (736)	**-0.46**	-0.09	-0.01
Sitta europaea (1841)	**-0.47**	0.03	**-0.51**
Spinus spinus (848)	-0.07	**0.18**	**0.17**
Sturnus vulgaris (353)	**-0.56**	-0.29	**0.46**
Sylvia atricapilla (1904)	**-0.46**	**0.13**	**-0.24**
Sylvia borin (576)	**-0.49**	**0.14**	**0.23**
Sylvia communis (143)	-0.39	0.36	**0.71**
Sylvia curruca (753)	**0.26**	**0.35**	**0.28**
Tichodroma muraria (1318)	**0.86**	**-0.27**	**-0.46**
Troglodytes troglodytes (2903)	**-0.27**	**0.47**	0.01
Turdus merula (2938)	**-0.39**	**0.18**	-0.04
Turdus philomelos (1209)	**-0.37**	**0.56**	-0.06
Turdus pilaris (1270)	0.04	**0.2**	**0.29**
Turdus torquatus (1665)	**0.51**	**0.64**	**0.36**
Turdus viscivorus (2585)	**-0.11**	**0.43**	**0.21**

Table 6 – Mean estimated parameters on spatial covariates : PCA Axis 4 to 6. Significant parameters based on the 95% interval of credibility are in bold.

Species (Occurrences)	Urban wetlands	Woody Heaths	Deciduous forests
Acanthis flammea (464)	-0.26	-0.09	0.13
Acrocephalus palustris (138)	-0.24	-0.04	-0.25
Aegithalos caudatus (1599)	0	**0.07**	**-0.2**
Alauda arvensis (1068)	0.11	**-0.34**	-0.01
Anthus spinoletta (1934)	0.02	**0.1**	0.01
Anthus trivialis (1292)	**-0.43**	**-0.37**	**0.14**
Bombycilla garrulus (146)	NA	NA	NA
Carduelis carduelis (1549)	**0.15**	-0.01	**-0.08**
Carduelis citrinella (730)	-0.02	0.04	0.03
Certhia brachydactyla (449)	0.05	0.03	**-0.22**
Certhia familiaris (984)	-0.27	**-0.56**	0.08
Chloris chloris (668)	**0.23**	-0.01	**-0.17**
Cinclus cinclus (1887)	**0.14**	0.04	**-0.16**
Coccothraustes coccothraustes (486)	**0.15**	0	**-0.1**
Corvus corone (1745)	-0.02	-0.02	**-0.11**
Corvus corone cornix (187)	-0.09	0.08	**-0.41**
Corvus monedula (152)	-0.1	**0.67**	-0.23
Cyanistes caeruleus (1892)	-0.06	0.05	**-0.12**
Delichon urbicum (734)	-0.02	**0.26**	0.04
Emberiza cia (1548)	**-0.2**	**0.16**	-0.05
Emberiza cirlus (202)	-0.19	0	-0.06
Emberiza citrinella (1734)	-0.11	**-0.18**	**-0.18**
Emberiza hortulana (134)	-0.29	0.09	-0.1
Erithacus rubecula (3354)	**-0.1**	0.01	-0.01
Ficedula hypoleuca (273)	0.09	0.09	**-0.13**
Fringilla coelebs (5447)	**-0.12**	**-0.1**	**0.07**
Fringilla montifringilla (551)	-0.09	-0.02	-0.08
Garrulus glandarius (2201)	**-0.16**	-0.03	**-0.06**
Hirundo rustica (642)	**0.27**	-0.07	**-0.14**
Lanius collurio (834)	-0.14	**-0.2**	**-0.14**
Linaria cannabina (1369)	0.08	0.04	**0.12**
Lophophanes cristatus (2160)	-0.11	**-0.15**	**0.24**
Loxia curvirostra (1890)	-0.23	**-0.46**	**0.51**
Lullula arborea (321)	**-0.21**	-0.05	0.01
Luscinia megarhynchos (376)	-0.14	-0.05	-0.11
Monticola saxatilis (566)	**-0.61**	0.09	**0.35**
Montifringilla nivalis (999)	**-0.18**	-0.09	0.01
Motacilla alba (1088)	**0.34**	-0.02	**-0.16**
Motacilla cinerea (697)	**0.25**	0.07	**-0.2**
Motacilla flava (144)	**0.83**	**-0.72**	-0.02
Nucifraga caryocatactes (2275)	**0.15**	-0.01	**0.13**

Oenanthe oenanthe (2263)	**-0.15**	0.06	0.03
Parus major (3165)	-0.03	**0.11**	**-0.17**
Passer domesticus (947)	**0.38**	**-0.3**	-0.05
Passer montanus (209)	0.07	-0.27	0
Periparus ater (3595)	**-0.23**	**-0.24**	**0.26**
Petronia petronia (197)	0.1	-0.32	**-0.33**
Phoenicurus ochruros (4183)	**-0.15**	**0.11**	-0.04
Phoenicurus phoenicurus (668)	**0.25**	0	**-0.16**
Phylloscopus bonelli (1668)	-0.06	**0.14**	**-0.15**
Phylloscopus collybita (2944)	0	**0.1**	**-0.14**
Pica pica (1061)	-0.02	**-0.12**	**-0.12**
Poecile montanus (2433)	-0.17	**-0.37**	**0.19**
Poecile palustris (774)	-0.05	0.05	**-0.11**
Prunella collaris (1775)	-0.08	**0.18**	0.09
Prunella modularis (1386)	**-0.17**	0.02	**0.22**
Ptyonoprogne rupestris (1695)	-0.07	**0.32**	-0.03
Pyrrhula pyrrhula (1816)	-0.1	**-0.24**	**0.14**
Regulus ignicapilla (686)	**-0.56**	**-0.42**	**0.35**
Regulus regulus (1030)	-0.22	**-0.24**	**0.3**
Saxicola rubetra (944)	-0.07	**-0.17**	**-0.22**
Saxicola rubicola (313)	**-0.21**	-0.1	**-0.26**
Serinus serinus (736)	**0.14**	**0.11**	-0.08
Sitta europaea (1841)	0	**-0.08**	**-0.16**
Spinus spinus (848)	0.09	0.04	**0.13**
Sturnus vulgaris (353)	**0.32**	**-0.67**	0.03
Sylvia atricapilla (1904)	0.01	**0.16**	**-0.09**
Sylvia borin (576)	0	0.06	**-0.21**
Sylvia communis (143)	**-0.3**	0.09	-0.1
Sylvia curruca (753)	**-0.49**	-0.03	**0.2**
Tichodroma muraria (1318)	**-0.16**	**0.4**	**0.13**
Troglodytes troglodytes (2903)	**-0.23**	**-0.13**	0.05
Turdus merula (2938)	**-0.07**	**0.05**	**-0.05**
Turdus philomelos (1209)	0.03	**-0.26**	0.05
Turdus pilaris (1270)	**-0.23**	**-0.15**	0.06
Turdus torquatus (1665)	**-0.6**	**-0.3**	**0.41**
Turdus viscivorus (2585)	**-0.22**	**-0.19**	**0.08**

Table 7 – Mean estimated parameters on spatio-temporal covariates : anomalies of maximum temprature and anomalies of precipitation. Significant parameters based on the 95% interval of credibility are in bold.

Species (Occurrences)	Anomalies of Tmax	Anomalies of Precipitation
Acanthis flammea (464)	-0.002	-0.0215
Acrocephalus palustris (138)	-0.0044	**0.2126**
Aegithalos caudatus (1599)	0.001	**-0.0633**
Alauda arvensis (1068)	0.003	**0.1266**
Anthus spinoletta (1934)	0.0026	0.0376
Anthus trivialis (1292)	0.0019	0.0237
Bombycilla garrulus (146)	NA	NA
Carduelis carduelis (1549)	6e-04	-0.0013
Carduelis citrinella (730)	-0.0019	**-0.0407**
Certhia brachydactyla (449)	-0.001	-0.0068
Certhia familiaris (984)	0.0012	**-0.0321**
Chloris chloris (668)	**0.0071**	**0.1904**
Cinclus cinclus (1887)	-5e-04	**-0.0223**
Coccothraustes coccothraustes (486)	-0.0031	**-0.272**
Corvus corone (1745)	-0.0016	**-0.0549**
Corvus corone cornix (187)	-0.0052	**-0.0928**
Corvus monedula (152)	-0.0061	-5e-04
Cyanistes caeruleus (1892)	1e-04	**-0.0823**
Delichon urbicum (734)	5e-04	**0.1054**
Emberiza cia (1548)	-5e-04	0.0086
Emberiza cirlus (202)	0.0024	**0.0605**
Emberiza citrinella (1734)	-0.0012	-0.0128
Emberiza hortulana (134)	0.0097	**0.2859**
Erithacus rubecula (3354)	-0.0013	-0.0195
Ficedula hypoleuca (273)	-5e-04	0.0073
Fringilla coelebs (5447)	-0.0011	-0.0236
Fringilla montifringilla (551)	0.0031	**-0.2194**
Garrulus glandarius (2201)	2e-04	0.0014
Hirundo rustica (642)	**0.0073**	0.0208
Lanius collurio (834)	**0.0065**	**0.2762**
Linaria cannabina (1369)	-0.0021	**0.0514**
Lophophanes cristatus (2160)	-2e-04	-0.0279
Loxia curvirostra (1890)	0.0013	**-0.0489**
Lullula arborea (321)	3e-04	0.0426
Luscinia megarhynchos (376)	**-0.0094**	0.1224
Monticola saxatilis (566)	0.006	**0.1575**
Montifringilla nivalis (999)	0.0014	**-0.1305**
Motacilla alba (1088)	-0.0024	0.0163
Motacilla cinerea (697)	-0.0032	**0.0632**
Motacilla flava (144)	-0.0051	0.1618

Nucifraga caryocatactes (2275)	0	4e-04
Oenanthe oenanthe (2263)	-6e-04	**0.129**
Parus major (3165)	2e-04	**-0.0695**
Passer domesticus (947)	-0.001	-0.0128
Passer montanus (209)	-0.0014	-0.0342
Periparus ater (3595)	4e-04	**-0.0424**
Petronia petronia (197)	-0.0036	**0.0778**
Phoenicurus ochruros (4183)	-1e-04	0.0478
Phoenicurus phoenicurus (668)	-0.0015	**-0.0212**
Phylloscopus bonelli (1668)	-4e-04	0.0714
Phylloscopus collybita (2944)	**-0.0031**	0.0105
Pica pica (1061)	**0.0026**	**-0.0426**
Poecile montanus (2433)	0.0013	**-0.0437**
Poecile palustris (774)	**0.0036**	**-0.1009**
Prunella collaris (1775)	0.0014	**-0.0971**
Prunella modularis (1386)	**-0.0047**	-0.0339
Ptyonoprogne rupestris (1695)	0.001	**0.0746**
Pyrrhula pyrrhula (1816)	9e-04	**-0.0381**
Regulus ignicapilla (686)	-0.004	-0.0081
Regulus regulus (1030)	0.002	**-0.0646**
Saxicola rubetra (944)	0.0027	**0.2046**
Saxicola rubicola (313)	0.0021	**0.1124**
Serinus serinus (736)	-7e-04	**0.1231**
Sitta europaea (1841)	**-0.0027**	**-0.0289**
Spinus spinus (848)	1e-04	**-0.1358**
Sturnus vulgaris (353)	0.005	0.0386
Sylvia atricapilla (1904)	**-0.0034**	0.0182
Sylvia borin (576)	-0.0041	**0.1405**
Sylvia communis (143)	**0.0193**	**0.2733**
Sylvia curruca (753)	0.0049	**0.1386**
Tichodroma muraria (1318)	-0.0019	**-0.0576**
Troglodytes troglodytes (2903)	-1e-04	0.0162
Turdus merula (2938)	6e-04	**-0.0262**
Turdus philomelos (1209)	-5e-04	-0.0198
Turdus pilaris (1270)	-0.0012	**-0.1565**
Turdus torquatus (1665)	-8e-04	-0.0144
Turdus viscivorus (2585)	**0.0014**	**-0.0779**

Table 8 – List of species removed from the habitat preference clustering based on the estimated mean parameters associated with the 6 spatial covariates corresponding to the first 6 axes of the principal component analysis detailed in Appendix 3.

Species (Occurrences	Reason
Acanthis flammea (464)	1 significant covariate
Acrocephalus palustris (138)	2 significant covariates
Bombycilla garrulus (146)	131 occurrences in 2005
Carduelis citrinella (730)	2 significant covariates
Cinclus cinclus (1887)	Poor AUCs
Corvus monedula (152)	1 significant covariate
Emberiza cirlus (202)	1 significant covariate
Emberiza hortulana (134)	1 significant covariate
Ficedula hypoleuca (273)	2 significant covariates
Fringilla montifringilla (551)	1 significant covariate
Luscinia megarhynchos (376)	1 significant covariate
Motacilla cinerea (697)	Poor AUCs
Passer montanus (209)	2 significant covariates
Sylvia communis (143)	2 significant covariates

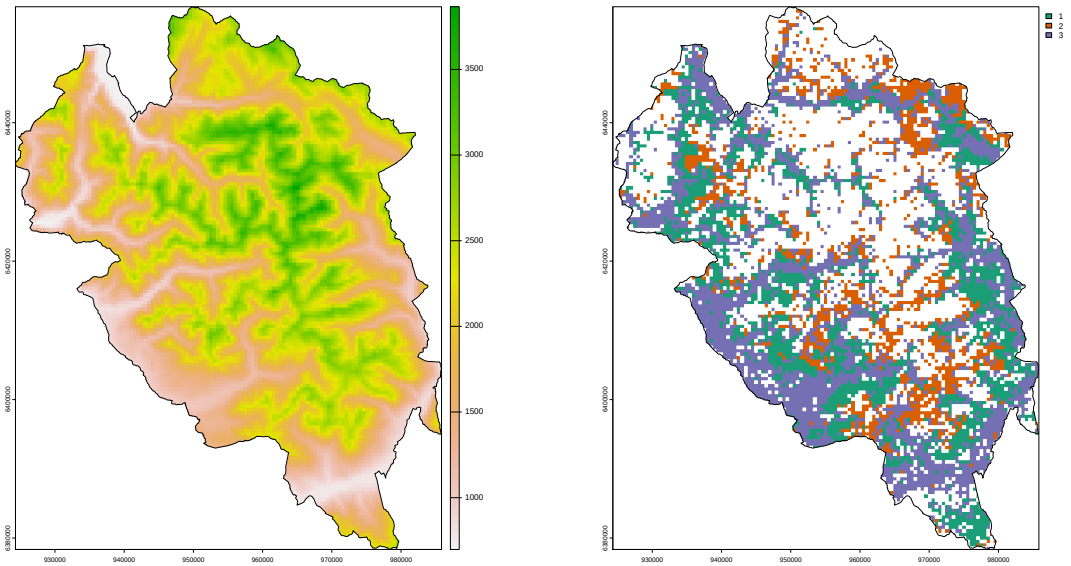

(a) (b)

Figure 14 – a) Map of elevation in the Écrins National Park on a 500m×500m regular grid. b) Map of clusters with the highest occurrences on a 500m×500m regular grid. The highest number of occurrences is computed from the 63 classified species: the 77th ones with more than 100 occurrences, excluding the species listed in Table 8. Cluster 1 is associated with forest species, Cluster 2 with high-elevation species, and Cluster 3 with species in the valleys.

900

7. Functionnal Principal Component Analysis

Table 9 – Scores associated with harmonics of the FPCA. The first harmonic is associated with species overrepresented in winter while the second is associated with species overrepresented in summer. The species are categorized by their main migratory status within the territory of the Écrins National Park, as provided by experts from the park

Species (Occurrences)	Winter	Summer	Migratory status
Acanthis flammea (464)	2.65	0.3	Resident
Acrocephalus palustris (138)	0.77	-0.57	Breeding migratory
Aegithalos caudatus (1599)	2.02	-1.13	Resident
Alauda arvensis (1068)	-4.67	-2.61	Breeding migratory
Anthus spinoletta (1934)	0.22	0.55	Breeding migratory
Anthus trivialis (1292)	-9.92	0.19	Breeding migratory
Bombycilla garrulus (146)	NA	NA	Wintering
Carduelis carduelis (1549)	1.15	-0.57	Resident
Carduelis citrinella (730)	1.63	-0.38	Resident
Certhia brachydactyla (449)	0.99	-0.56	Resident
Certhia familiaris (984)	0.94	-0.63	Resident
Chloris chloris (668)	1.66	0.86	Breeding migratory
Cinclus cinclus (1887)	NA	NA	Resident
Coccothraustes coccothraustes (486)	0.85	-3.22	Resident
Corvus corone (1745)	1.04	-0.6	Resident
Corvus corone cornix (187)	1.78	-0.23	Resident
Corvus monedula (152)	0.72	-0.75	Resident
Cyanistes caeruleus (1892)	1.46	-0.76	Resident
Delichon urbicum (734)	-3.29	2.17	Breeding migratory
Emberiza cia (1548)	1.04	0.11	Resident
Emberiza cirlus (202)	1.78	-0.08	Resident
Emberiza citrinella (1734)	0.42	0.91	Breeding migratory
Emberiza hortulana (134)	1.88	1.29	Breeding migratory
Erithacus rubecula (3354)	0.72	0.41	Resident
Ficedula hypoleuca (273)	-3.13	9.91	Breeding migratory
Fringilla coelebs (5447)	1.02	0.2	Resident
Fringilla montifringilla (551)	2.12	-1.67	Wintering
Garrulus glandarius (2201)	1.2	-0.41	Resident
Hirundo rustica (642)	-1.74	5.23	Breeding migratory
Lanius collurio (834)	2.03	1.75	Breeding migratory
Linaria cannabina (1369)	1.08	-0.43	Resident
Lophophanes cristatus (2160)	1.28	-1.79	Resident
Loxia curvirostra (1890)	1.71	-0.89	Resident
Lullula arborea (321)	-0.86	-1.1	Breeding migratory
Luscinia megarhynchos (376)	-13.95	-2.51	Breeding migratory
Monticola saxatilis (566)	0.08	1.21	Breeding migratory
Montifringilla nivalis (999)	1.4	-0.73	Resident

Motacilla alba (1088)	1.04	1.56	Breeding migratory
Motacilla cinerea (697)	NA	NA	Resident
Motacilla flava (144)	-3.02	0.21	Breeding migratory
Nucifraga caryocatactes (2275)	-2.61	-3.66	Resident
Oenanthe oenanthe (2263)	-6.52	-1.11	Breeding migratory
Parus major (3165)	1	-0.63	Resident
Passer domesticus (947)	1.47	-0.36	Resident
Passer montanus (209)	1.18	-0.57	Resident
Periparus ater (3595)	0.96	-0.66	Resident
Petronia petronia (197)	0.84	-0.64	Resident
Phoenicurus ochruros (4183)	0.62	0.91	Breeding migratory
Phoenicurus phoenicurus (668)	1.3	-0.41	Resident
Phylloscopus bonelli (1668)	-13.44	-1.74	Breeding migratory
Phylloscopus collybita (2944)	-0.82	3.58	Breeding migratory
Pica pica (1061)	1.52	-0.48	Resident
Poecile montanus (2433)	1.36	-0.67	Resident
Poecile palustris (774)	1.04	-0.59	Resident
Prunella collaris (1775)	1.21	-0.73	Resident
Prunella modularis (1386)	0.05	1.54	Resident
Ptyonoprogne rupestris (1695)	-0.63	1.47	Breeding migratory
Pyrrhula pyrrhula (1816)	1.49	-0.88	Resident
Regulus ignicapilla (686)	0.68	0.53	Breeding migratory
Regulus regulus (1030)	1.42	-0.87	Resident
Saxicola rubetra (944)	1.7	1.26	Breeding migratory
Saxicola rubicola (313)	1.6	0.25	Breeding migratory
Serinus serinus (736)	1.07	0.13	Breeding migratory
Sitta europaea (1841)	1.71	-1.13	Resident
Spinus spinus (848)	1.99	-1.15	Resident
Sturnus vulgaris (353)	-1.41	-2.53	Resident
Sylvia atricapilla (1904)	-0.15	2.25	Breeding migratory
Sylvia borin (576)	0.35	1.86	Breeding migratory
Sylvia communis (143)	1.41	0.58	Breeding migratory
Sylvia curruca (753)	-4.8	2.74	Breeding migratory
Tichodroma muraria (1318)	1.63	-0.52	Resident
Troglodytes troglodytes (2903)	1.08	-0.38	Resident
Turdus merula (2938)	0.94	-0.59	Resident
Turdus philomelos (1209)	0.28	1.46	Resident
Turdus pilaris (1270)	2.11	-2.43	Resident
Turdus torquatus (1665)	1.34	-0.43	Breeding migratory
Turdus viscivorus (2585)	0.94	-0.63	Resident

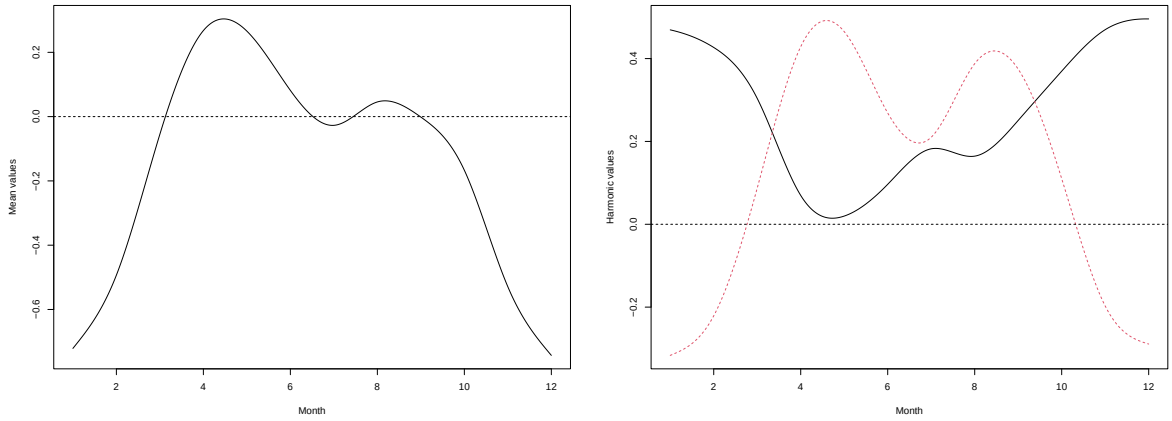

(a) (b)

Figure 15 – Figure 15a displays the mean component of the spatial means of the month-dependent spatio-temporal Gaussian field W_i^m. Figure 15b displays the first two harmonics from the Functional Principal Component Analysis (FPCA) of the spatial means of the month-dependent spatio-temporal Gaussian field W_i^m. The black curve represents the first harmonic, explaining 61% of the variance in intra-annual variations. The red dotted curve represents the second harmonic, explaining 22% of the variance in intra-annual variations.

901

8. Inter-annual trends

Table 10 – Trends in relative abundance (RA) computed by the STOC and in target-group relative abundance (TGRA) in the Écrins National Park (ENP) for the period 2001-2019. The trends are expressed as percentage of variations, as developed in the section "Materials and Methods – Validation and post-processing – Inter-annual effects". Credibility intervals are provided. The last column contains the differences between the median of these two metrics.

Species (Occurrences)	STOC RA	ENP TGRA	Differences
Acanthis flammea (464)	NA	-5.3 [-28.8, 25.8]	NA
Acrocephalus palustris (138)	-13.8 [-49.8, 47.8]	0 [-1.6, 1.7]	13.8
Aegithalos caudatus (1599)	NA	22.6 [5.9, 42.8]	NA
Alauda arvensis (1068)	-22.6 [-26, -19.1]	0 [-1.7, 1.8]	22.6
Anthus spinoletta (1934)	NA	-11.1 [-24.3, 4.1]	NA
Anthus trivialis (1292)	-19.3 [-27.4, -10.3]	-0.2 [-1.9, 1.7]	19.1
Bombycilla garrulus (146)	NA	NA	NA
Carduelis carduelis (1549)	-30.8 [-36.3, -25]	0 [-1.7, 1.7]	30.8
Carduelis citrinella (730)	NA	-18.1 [-34.8, 1.2]	NA
Certhia brachydactyla (449)	12.6 [4.3, 21.5]	0.1 [-1.7, 2]	-12.5
Certhia familiaris (984)	-9.3 [-43.1, 44.5]	0 [-1.7, 1.7]	9.3
Chloris chloris (668)	90.7 [65.4, 119.9]	11.3 [-10.9, 38.1]	-79.4
Cinclus cinclus (1887)	NA	NA	NA
Coccothraustes coccothraustes (486)	63 [24.8, 112.7]	-0.1 [-1.9, 1.6]	-63.1
Corvus corone (1745)	5.6 [0.8, 10.7]	-25.7 [-39.3, -10.7]	-31.3
Corvus corone cornix (187)	NA	-50.8 [-69.2, -24.1]	NA
Corvus monedula (152)	85.4 [57.5, 118.2]	-12 [-33.9, 17]	-97.4
Cyanistes caeruleus (1892)	14.6 [8.3, 21.2]	0 [-1.9, 2]	-14.6
Delichon urbicum (734)	-23.3 [-33.5, -11.6]	0 [-2, 1.7]	23.3
Emberiza cia (1548)	-45.4 [-68.1, -6.7]	-23.2 [-35, -11.7]	22.2
Emberiza cirlus (202)	-0.2 [-9.5, 10.1]	0.1 [-2, 2.1]	0.3
Emberiza citrinella (1734)	-53.6 [-56.5, -50.5]	-0.2 [-1.7, 1.5]	53.4
Emberiza hortulana (134)	-78.3 [-78.3, -49.2]	-36.2 [-67, 5.7]	42.1
Erithacus rubecula (3354)	-9.2 [-13.1, -5.2]	29.7 [14.8, 45.9]	38.9
Ficedula hypoleuca (273)	19.1 [-47.1, 167.8]	-24.7 [-48.1, 9.1]	-43.8
Fringilla coelebs (5447)	4.9 [2.1, 7.7]	20 [7.6, 31.9]	15.1
Fringilla montifringilla (551)	NA	-34.4 [-51.1, -11.9]	NA
Garrulus glandarius (2201)	23.2 [13.3, 34]	-12.6 [-24.6, -0.9]	-35.8
Hirundo rustica (642)	-25.2 [-30.2, -19.8]	-5.4 [-19.8, 12.3]	19.8
Lanius collurio (834)	-1.7 [-15.8, 14.6]	-8.5 [-24.5, 9.7]	-6.8
Linaria cannabina (1369)	-8.1 [-17.7, 2.7]	0 [-2.1, 2.2]	8.1
Lophophanes cristatus (2160)	-7.8 [-25.6, 14.2]	38 [16.4, 60.4]	45.8
Loxia curvirostra (1890)	-3 [-50.3, 89.5]	-8.2 [-20.5, 6.4]	-5.2
Lullula arborea (321)	-6.3 [-16.4, 4.9]	-60 [-74.4, -40.7]	-53.7
Luscinia megarhynchos (376)	-2.4 [-6.6, 1.9]	0 [-1.8, 1.7]	2.4
Monticola saxatilis (566)	NA	-53.2 [-66.4, -38.5]	NA

Montifringilla nivalis (999)	NA	-24.7 [-38.4, -7.5]	NA
Motacilla alba (1088)	4.3 [-5.6, 15.3]	-0.1 [-1.7, 1.5]	-4.4
Motacilla cinerea (697)	7.1 [-22.9, 48.9]	NA	NA
Motacilla flava (144)	-13 [-25.7, 1.8]	-62 [-81, -38]	-49
Nucifraga caryocatactes (2275)	NA	-21.5 [-32.6, -8.9]	NA
Oenanthe oenanthe (2263)	13.4 [-42.4, 123.3]	0.1 [-1.8, 1.9]	-13.3
Parus major (3165)	7.4 [3.2, 11.8]	6.5 [-7.6, 21.5]	-0.9
Passer domesticus (947)	-4.6 [-8.9, 0]	-4 [-21.8, 16.9]	0.6
Passer montanus (209)	-60.2 [-68.7, -49.3]	-0.1 [-1.9, 1.8]	60.1
Periparus ater (3595)	1.5 [-11.6, 16.6]	22.9 [10.5, 38.1]	21.4
Petronia petronia (197)	NA	-26.2 [-53.8, 19]	NA
Phoenicurus ochruros (4183)	2.9 [-4, 10.4]	12.2 [0.4, 24.9]	9.3
Phoenicurus phoenicurus (668)	-50 [-53.1, -46.7]	0 [-1.9, 1.8]	50
Phylloscopus bonelli (1668)	52.5 [29.3, 80]	68.1 [39.8, 103.9]	15.6
Phylloscopus collybita (2944)	-11 [-14.3, -7.6]	19 [4.2, 35.9]	30
Pica pica (1061)	14.5 [6.9, 22.5]	0.1 [-1.7, 1.8]	-14.4
Poecile montanus (2433)	-48.8 [-65.9, -22.9]	31.6 [14.2, 52.6]	80.4
Poecile palustris (774)	9.1 [-10, 32.1]	-0.1 [-1.8, 1.9]	-9.2
Prunella collaris (1775)	NA	-26.6 [-38, -13]	NA
Prunella modularis (1386)	-26.5 [-32, -20.6]	0.1 [-1.7, 1.8]	26.6
Ptyonoprogne rupestris (1695)	NA	-0.1 [-1.9, 1.9]	NA
Pyrrhula pyrrhula (1816)	-33.2 [-46.5, -16.4]	-12 [-26.1, 1.9]	21.2
Regulus ignicapilla (686)	79 [54.5, 107.3]	168.7 [92.5, 285.5]	89.7
Regulus regulus (1030)	-43.7 [-51.6, -34.4]	0 [-1.6, 1.8]	43.7
Saxicola rubetra (944)	-60.3 [-72.8, -42.1]	0 [-1.7, 1.8]	60.3
Saxicola rubicola (313)	-22 [-28.8, -14.5]	-32.1 [-52.8, -8.4]	-10.1
Serinus serinus (736)	-41.7 [-46.5, -36.6]	-0.1 [-1.8, 1.9]	41.6
Sitta europaea (1841)	1.3 [-9.2, 12.9]	0 [-2, 1.8]	-1.3
Spinus spinus (848)	NA	3.1 [-21.7, 35.1]	NA
Sturnus vulgaris (353)	22.4 [12.4, 33.2]	-0.1 [-1.9, 1.6]	-22.5
Sylvia atricapilla (1904)	29.6 [25.9, 33.4]	70.6 [45.3, 103.8]	41
Sylvia borin (576)	-32.7 [-39.4, -25.2]	-18.3 [-37.4, 6.6]	14.4
Sylvia communis (143)	-12.5 [-17.9, -6.8]	0 [-1.9, 1.7]	12.5
Sylvia curruca (753)	-7.5 [-31.7, 25.3]	0.2 [-1.6, 2]	7.7
Tichodroma muraria (1318)	NA	-41.5 [-51.6, -28.1]	NA
Troglodytes troglodytes (2903)	-20 [-22.9, -17.1]	11.1 [-2.1, 26]	31.1
Turdus merula (2938)	7 [3.9, 10.2]	8.7 [-6.3, 25.1]	1.7
Turdus philomelos (1209)	-0.9 [-5.9, 4.3]	30.9 [7.5, 61]	31.8
Turdus pilaris (1270)	-32.4 [-65.5, 32.8]	-42.1 [-54.7, -25.2]	-9.7
Turdus torquatus (1665)	NA	0 [-2, 2.3]	NA
Turdus viscivorus (2585)	-0.2 [-9.8, 10.5]	-7.1 [-14.6, 1.8]	-6.9